Cryo electron tomography

Cryo-EM SPA

1 view, multiple copies of the object

Cryo-ET

1 object, multiple views

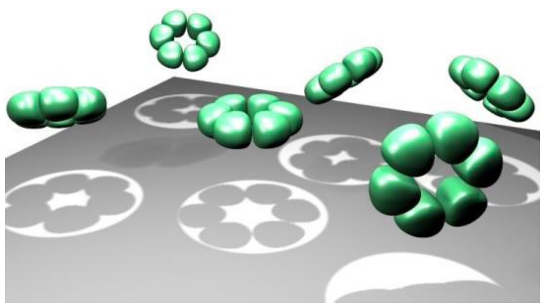

o.lambert@cbmn.u-bordeaux.fr

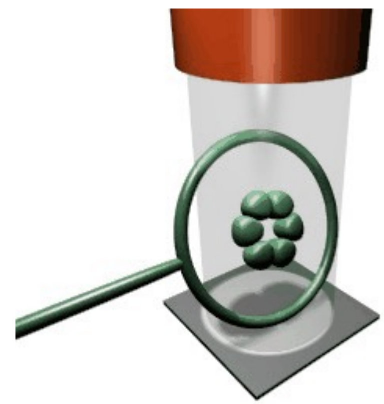

Amélie Leforestier
Laboratoire de Physique des Solides, Orsay

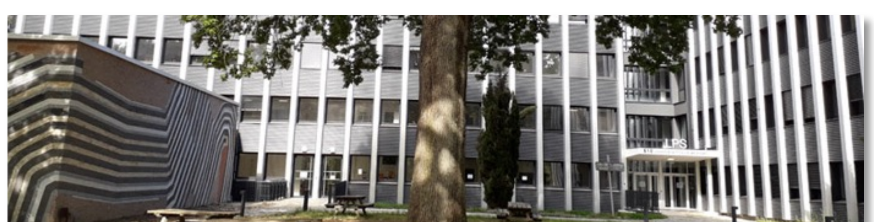

université
PARIS-SACLAY

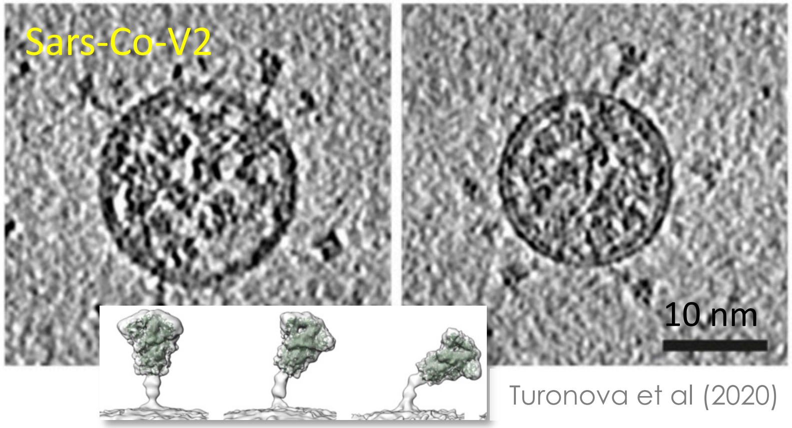

Turonova et al (2020)

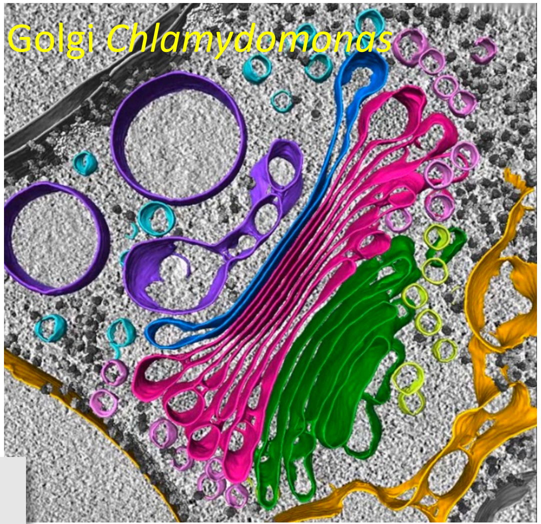

Engel et al (2016)

Unique objects

- cells & tissues
- many viruses (HIV, Ebola, Sars-Co-V2, …)
- complex macromolecular assemblies
- liposomes, cubosomes, vesicles, NPs …

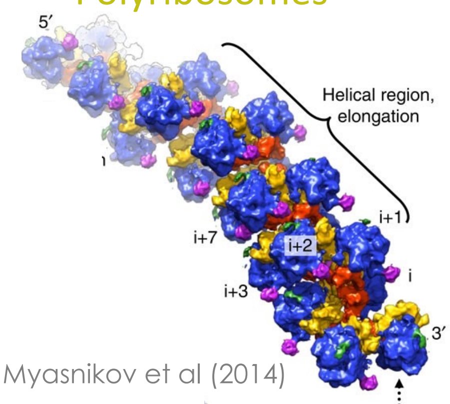

Myasnikov et al (2014)

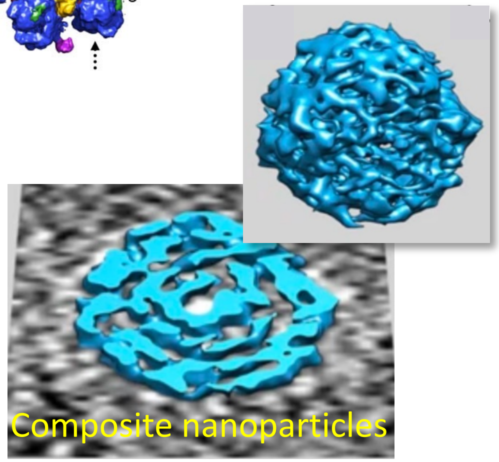

Kochovsky et al (2020)

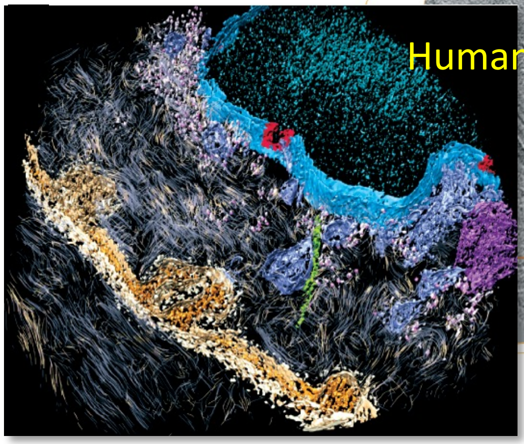

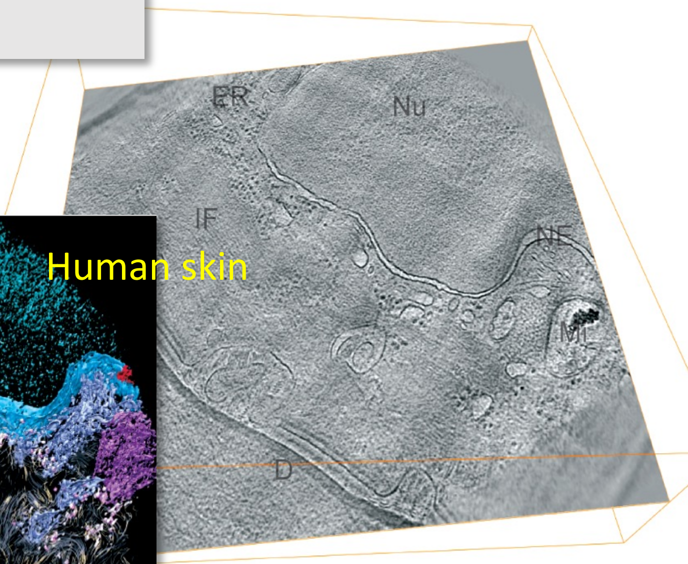

Al-Amoudi et al (2007)

Cryo electron tomography

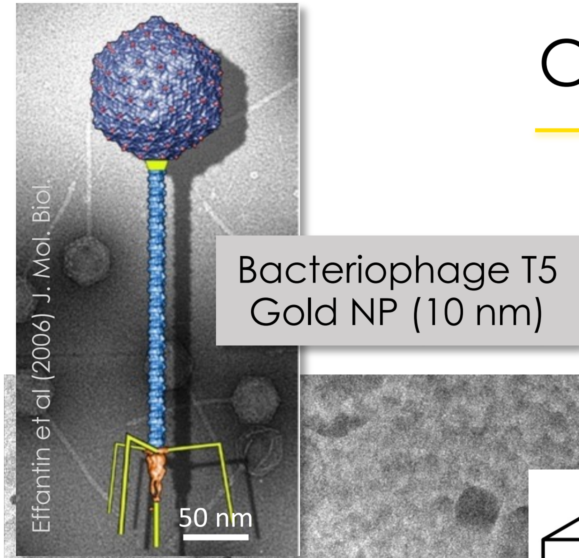

τόμος: "slice, section"

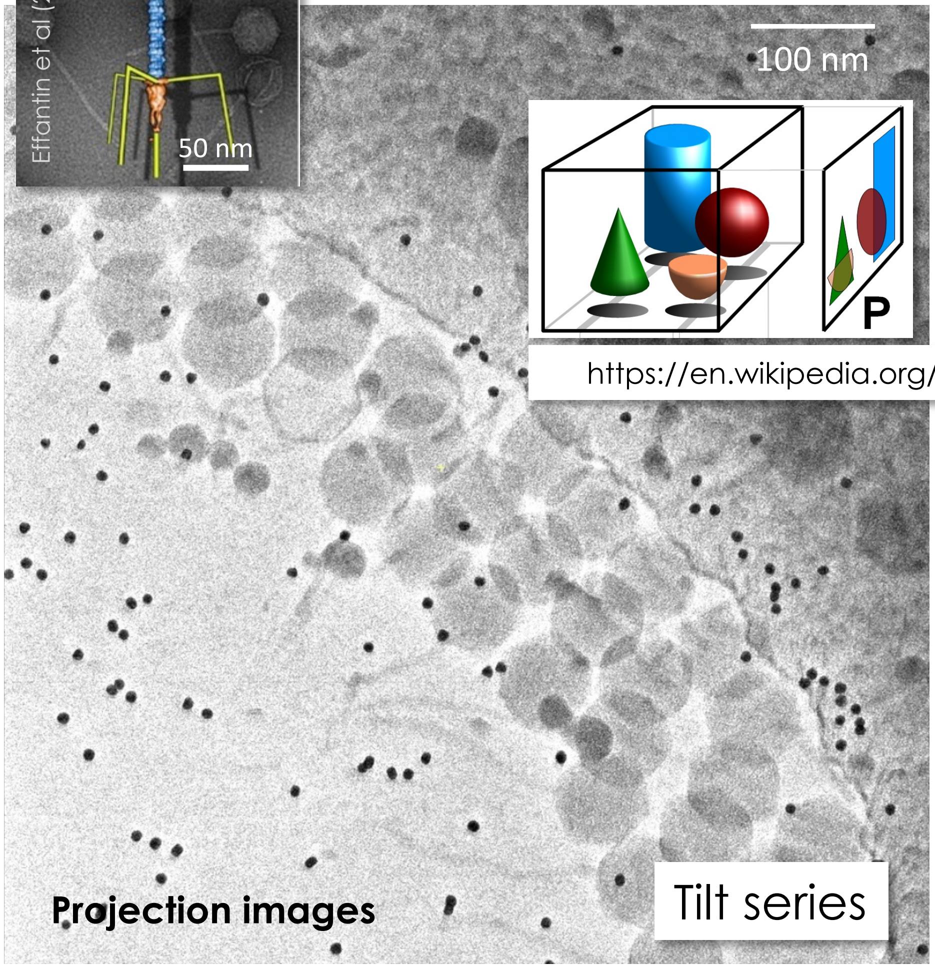

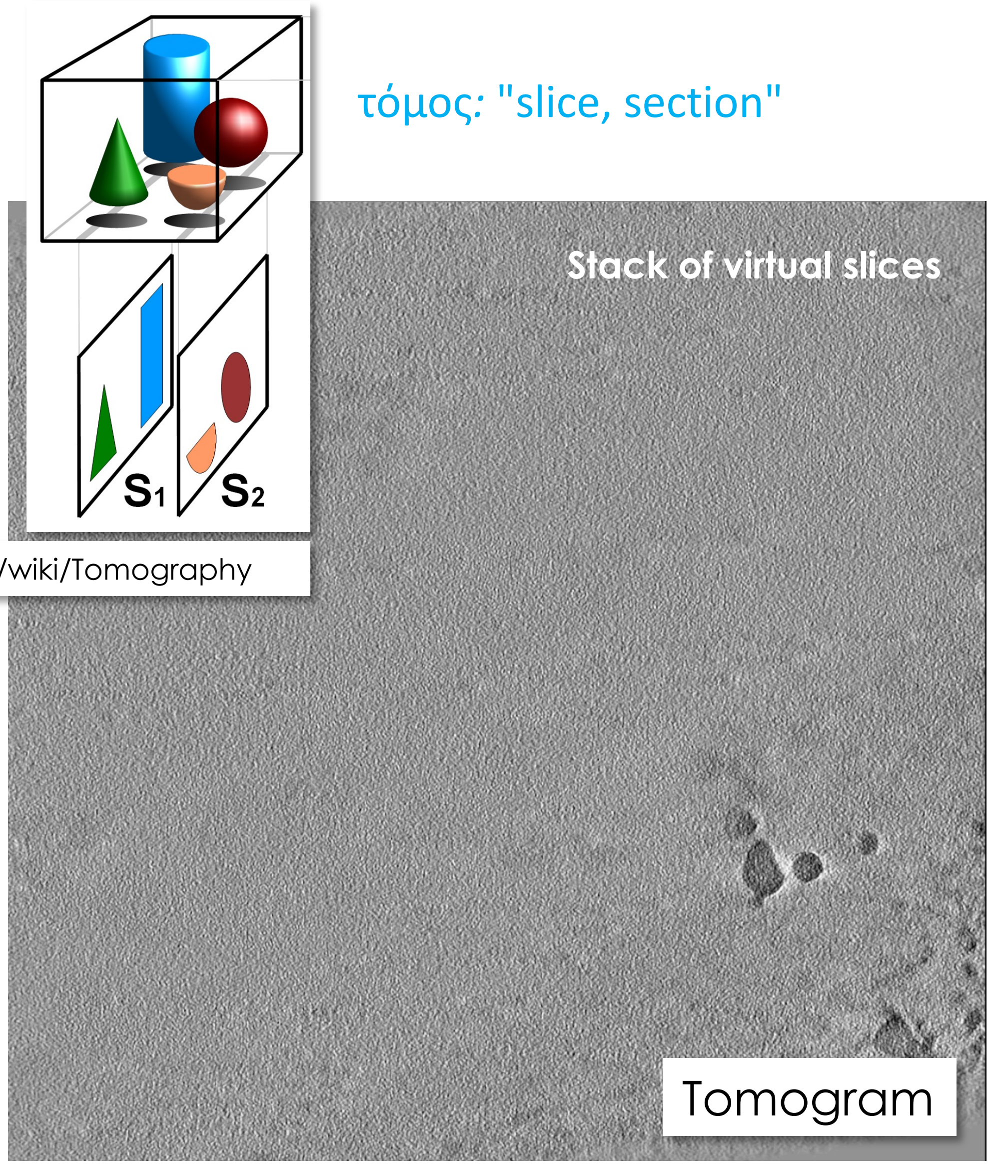

https://en.wikipedia.org/wiki/Tomography

Titan Krios IGBMC, Strasbourg

Cryo electron tomography

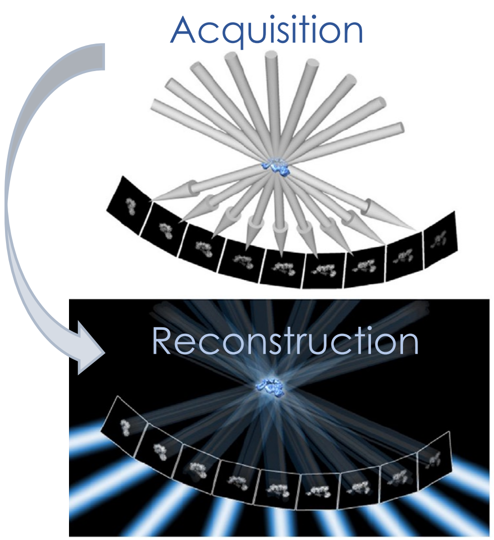

R.I. Koning et al. / Annals of Anatomy 217 (2018) 82–96

- Tilt series acquisition
  (electron dose, acquisition schemes)
- CTF-correction (2D, 3D)
- Alignment
- Tomogram reconstruction
- Tomogram visualization
- Segmentation
- STA

- Missing information

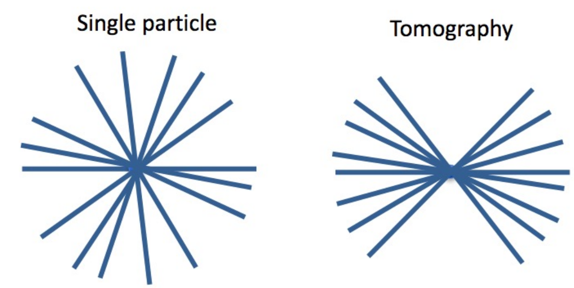

Missing information: tilt range limitation

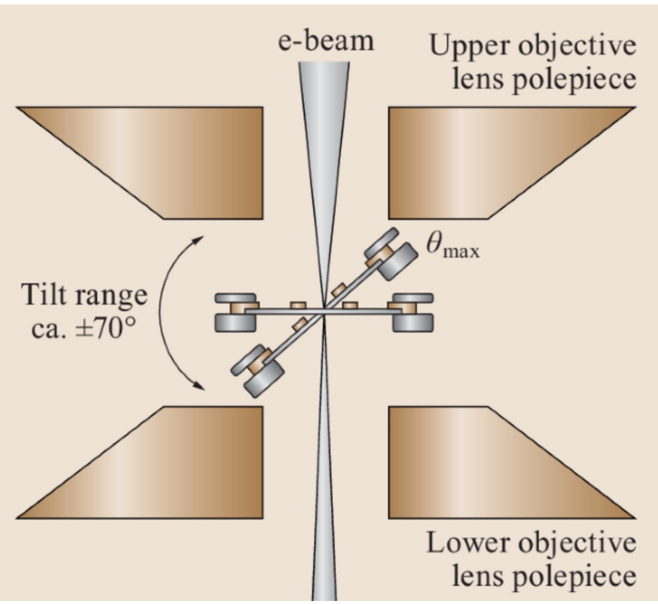

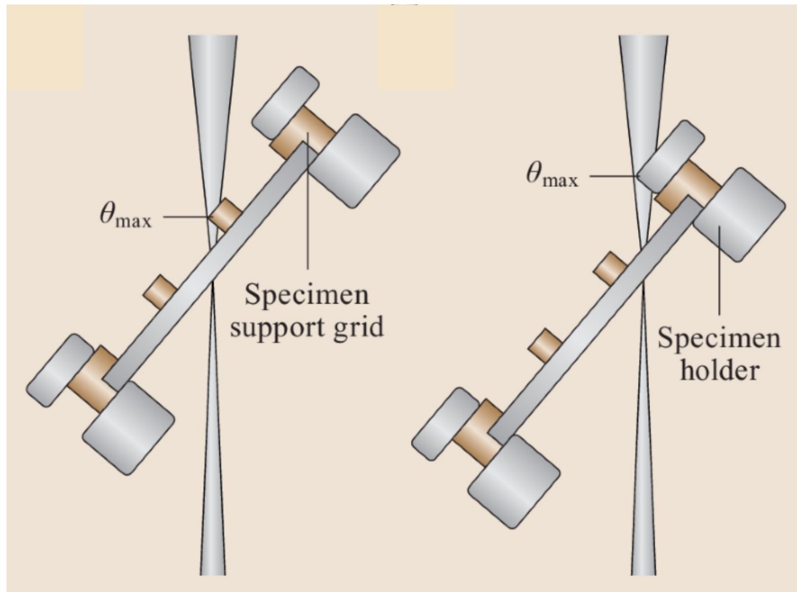

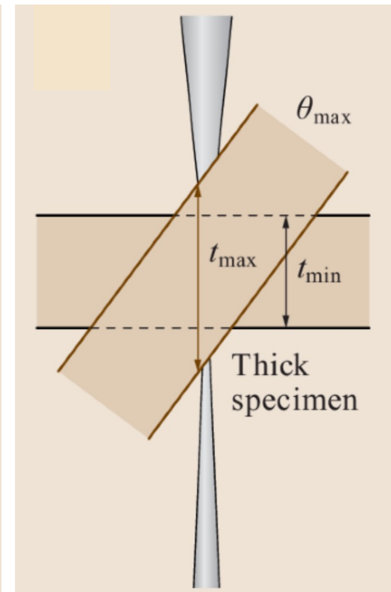

High tilt polepieces

Tomography holders

Leary & Midgley (2019) Electron tomography in material sciences, Springer Handbook of microscopy, pp 1279-1329

Missing information

Fourier space partially and inhomogeneously filled

Central slice theorem

each projection, of an object of diameter D, is a central section in Fourier space of thickness $1/D$.

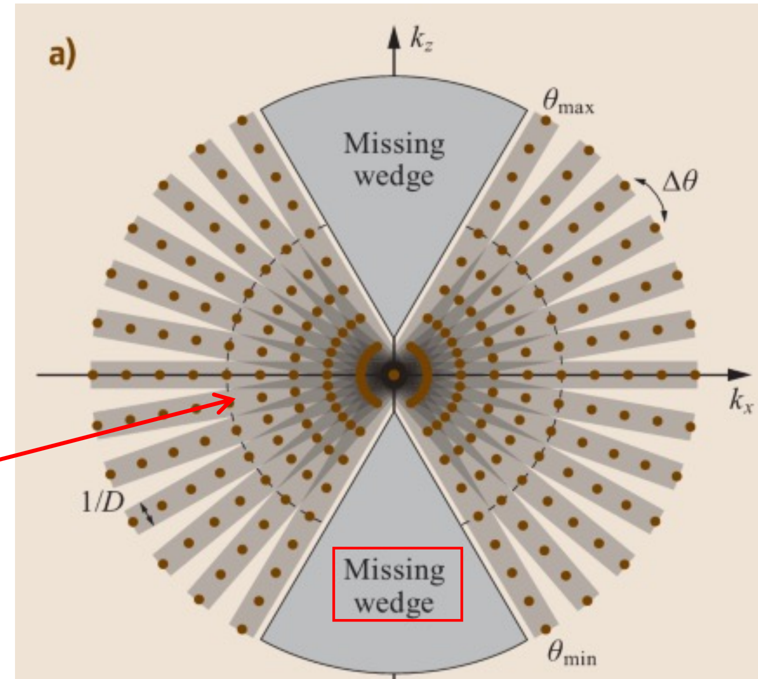

Leary & Midgley (2019) Springer Handbook of microscopy, pp 1279-1329

information from adjacent projections just overlaps

Crowther's criterion

$$R = \pi D / N$$

N ≈ number of images (angle increment)

Crowther, DeRosier & Klug (1970). Porc. Roy. Soc. Lond. A 317, 319-340.

Missing information

R.I. Koning et al. / Annals of Anatomy 217 (2018) 82–96

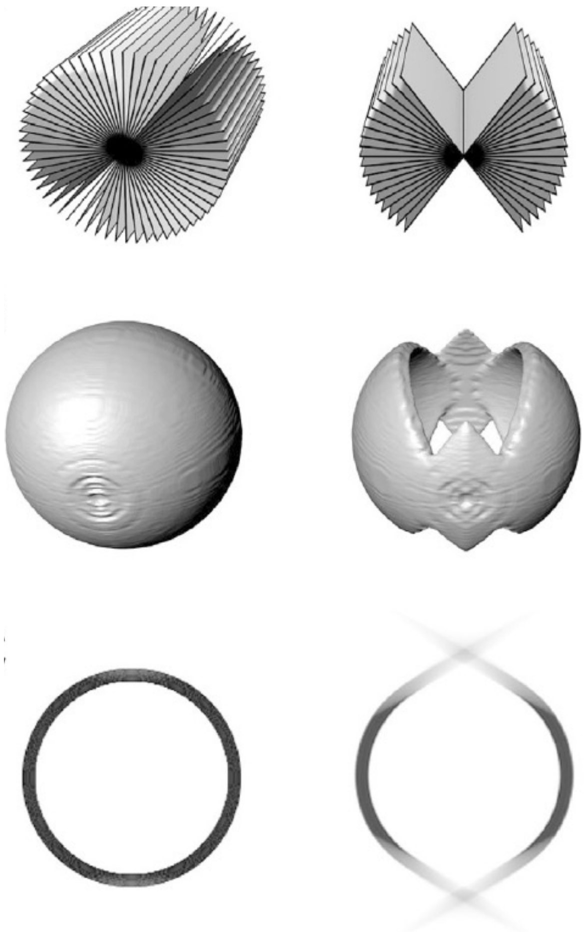

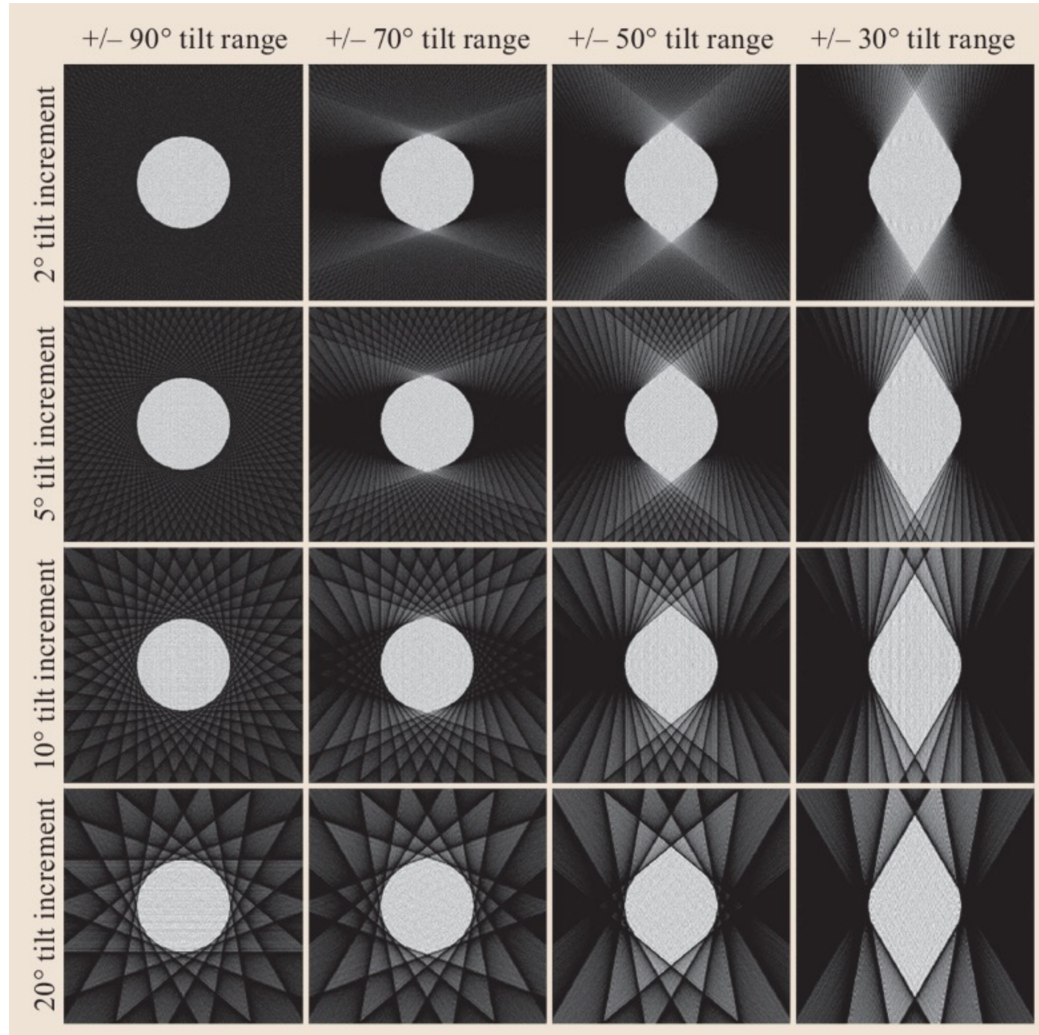

Missing information

R.I. Koning et al. / Annals of Anatomy 217 (2018) 82–96

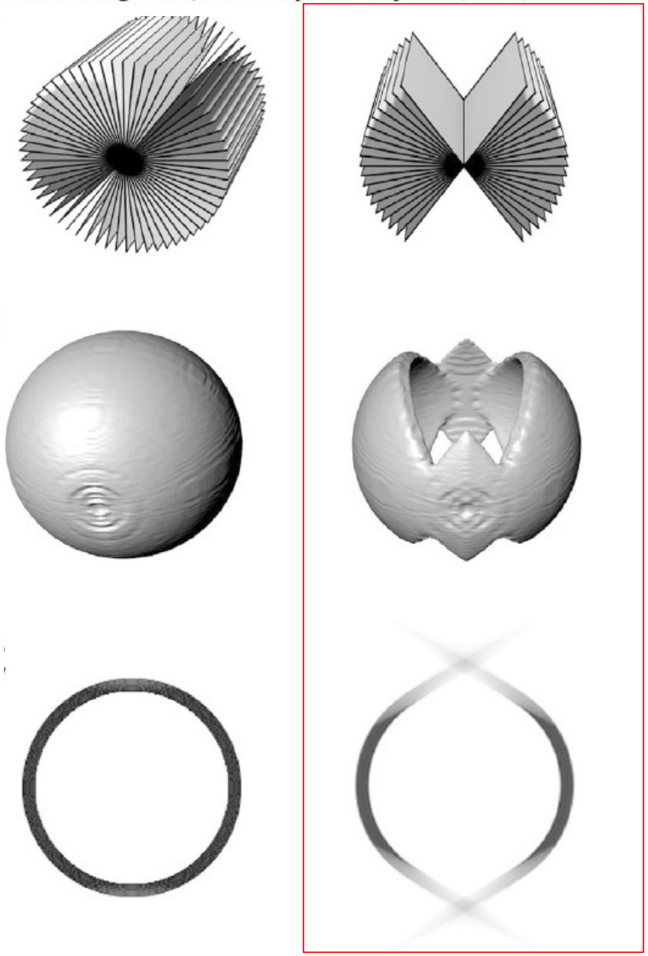

Bacteriophage T5
(empty capsid)

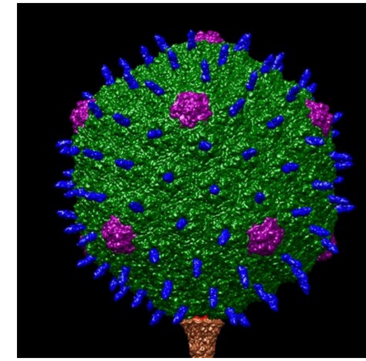

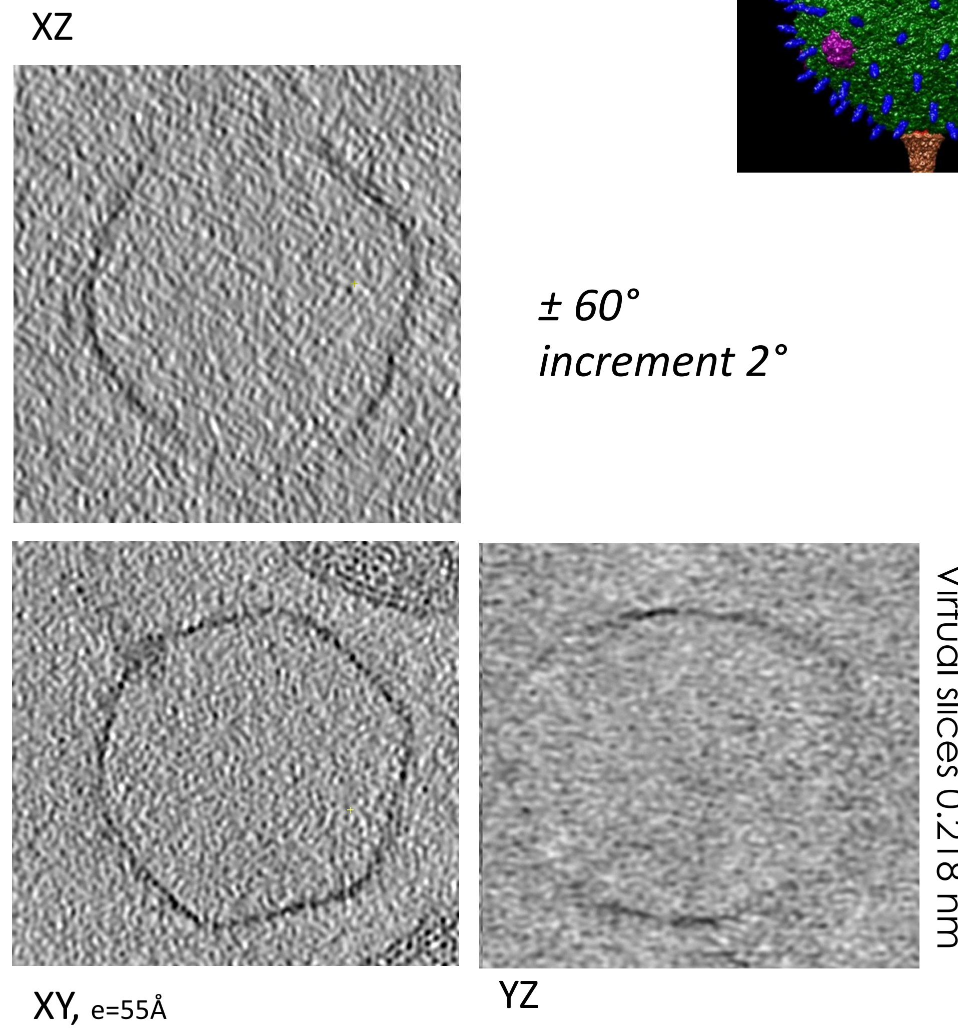

± 60°
increment 2°

Missing information

R.I. Koning et al. / Annals of Anatomy 217 (2018) 82–96

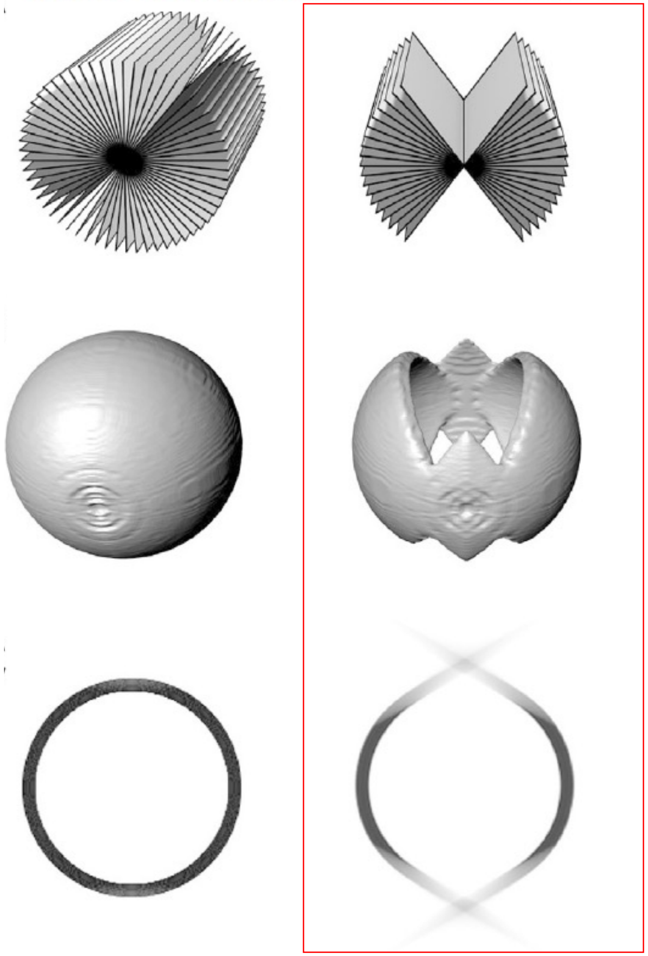

angular limitation
+ tilt axis orientation

Condensed DNA bundles
(hexagonal packing)

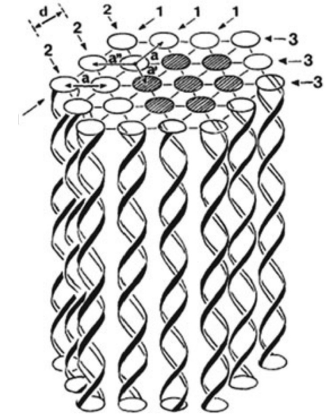

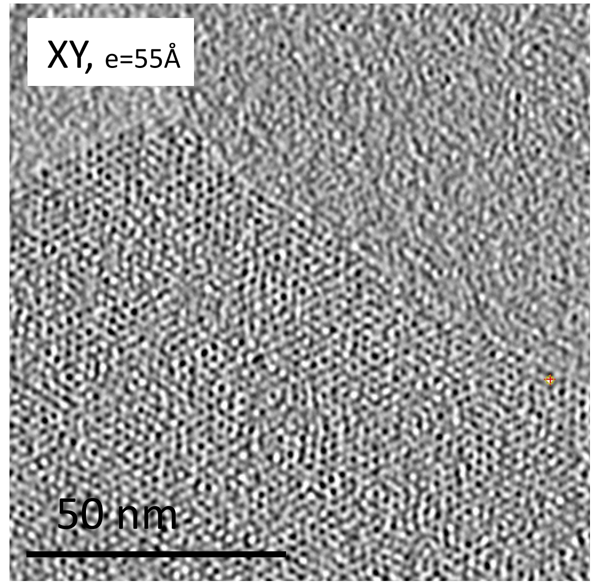

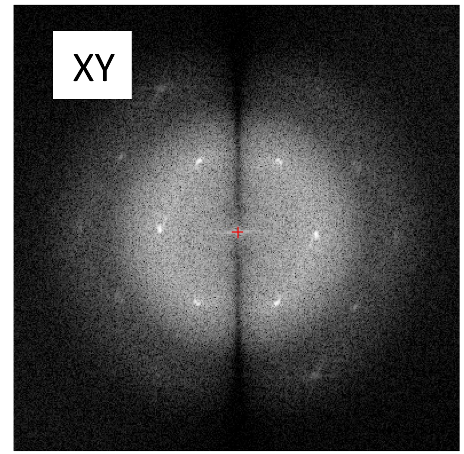

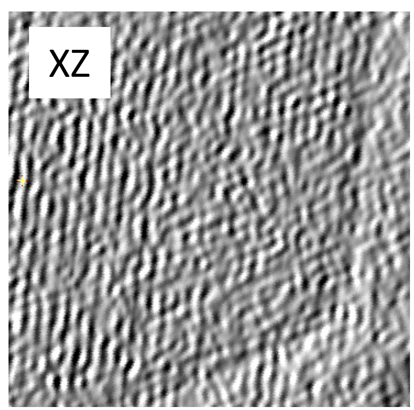

Virtual slices 0.218 nm

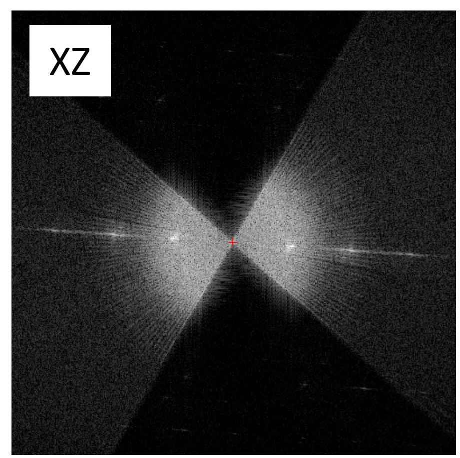

Missing information

R.I. Koning et al. / Annals of Anatomy 217 (2018) 82–96

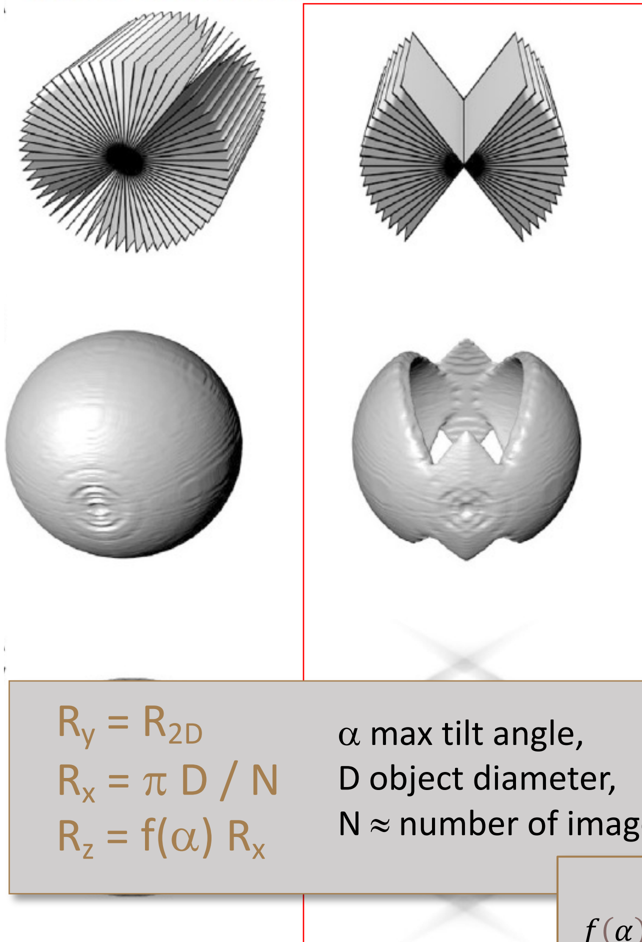

Condensed DNA bundles
(hexagonal packing)

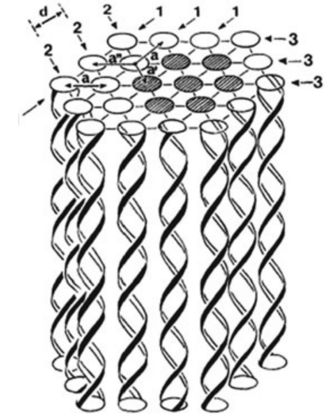

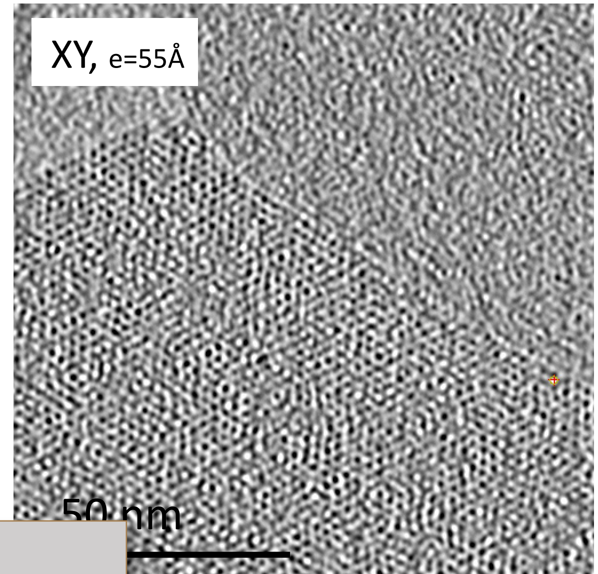

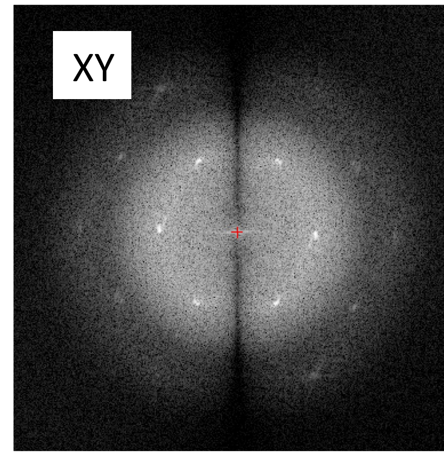

$R_y = R_{2D}$

$R_x = \pi D / N$

$R_z = f(\alpha) R_x$

α max tilt angle,
D object diameter,
N ≈ number of images (angles)

$$f(\alpha) = \sqrt{\frac{\alpha + \sin\alpha \cos\alpha}{\alpha - \sin\alpha \cos\alpha}}$$

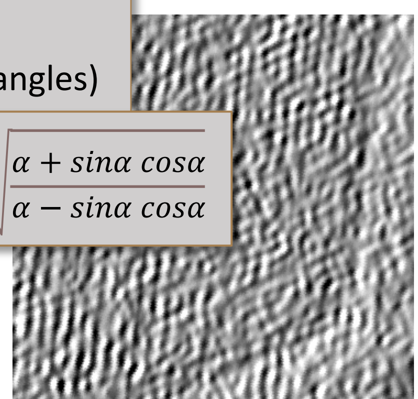

Virtual slices 0.218 nm

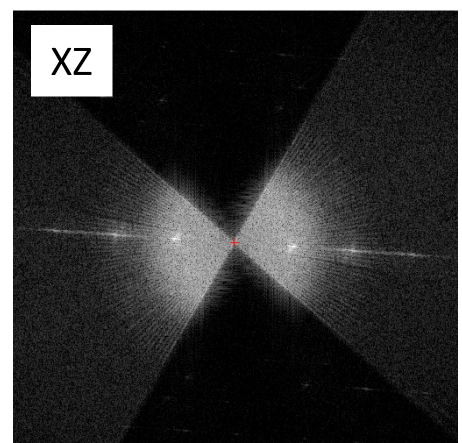

angular limitation
+ tilt axis orientation

anisotropic resolution

Missing information

R.I. Koning et al. / Annals of Anatomy 217 (2018) 82–96

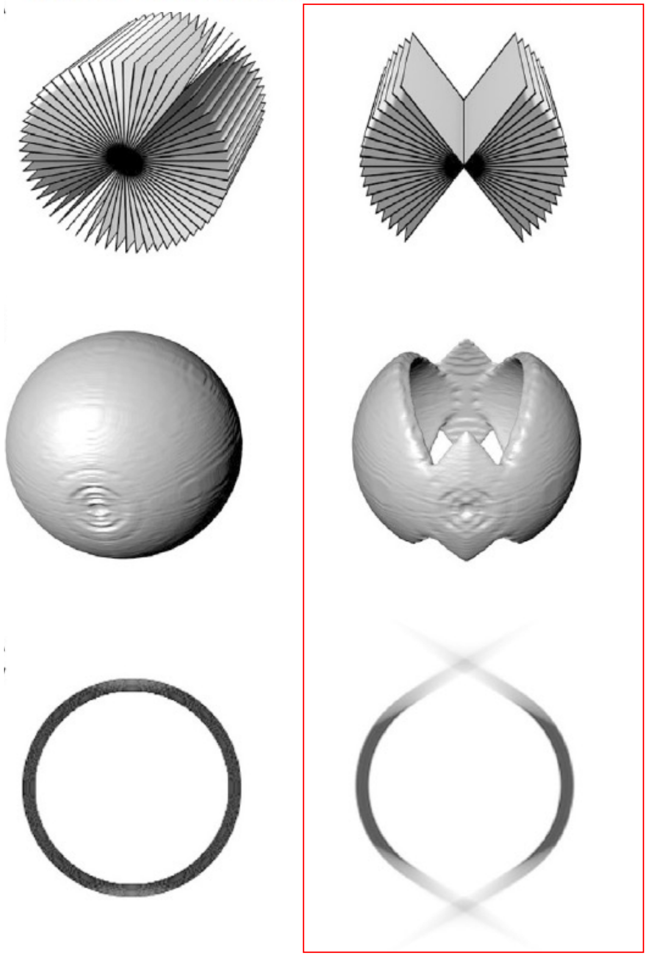

angular limitation
+ tilt axis orientation

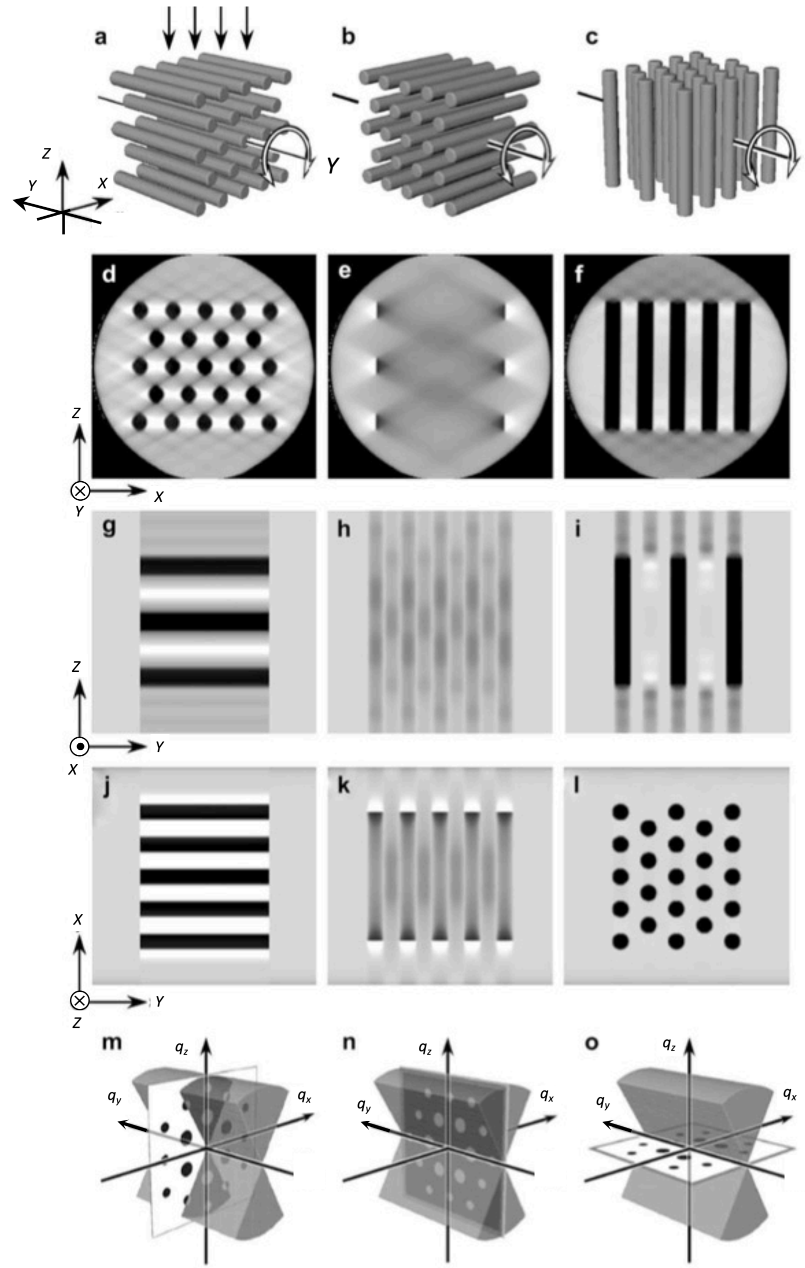

H. Jinnai, R.J. Spontak / Polymer 50 (2009) 1067–1087

Missing information: dual axis tomography

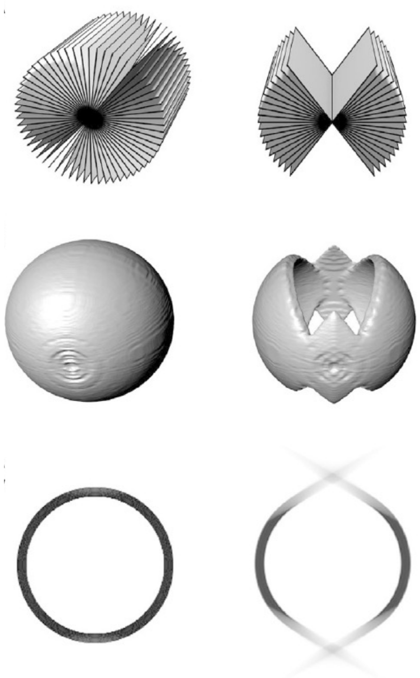

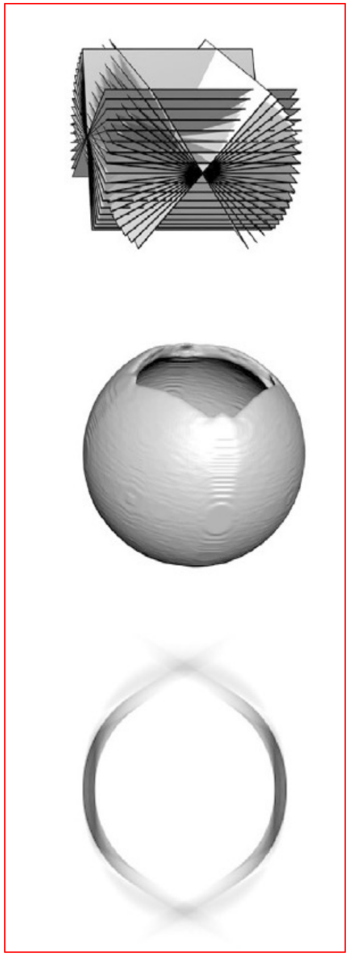

Microtubules

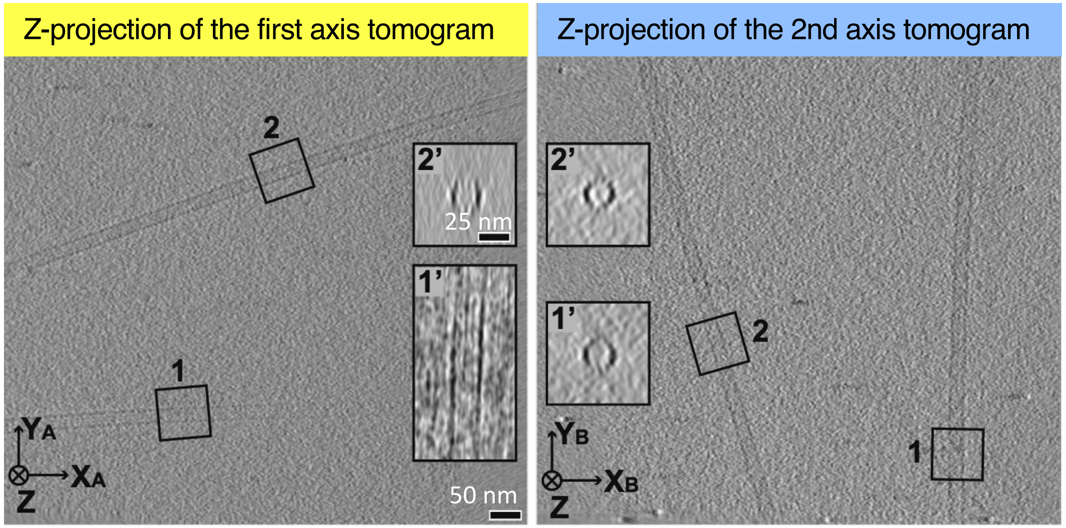

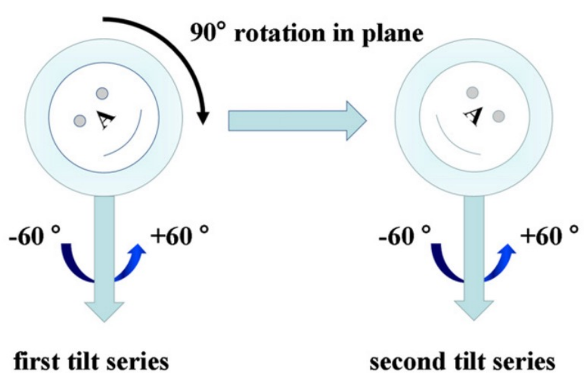

A. Guesdon et al. / Journal of Structural Biology 181 (2013) 169–178

A.G. Myasnikov et al. / Ultramicroscopy 126 (2013) 33–39

Missing information: dual axis tomography

Microtubules

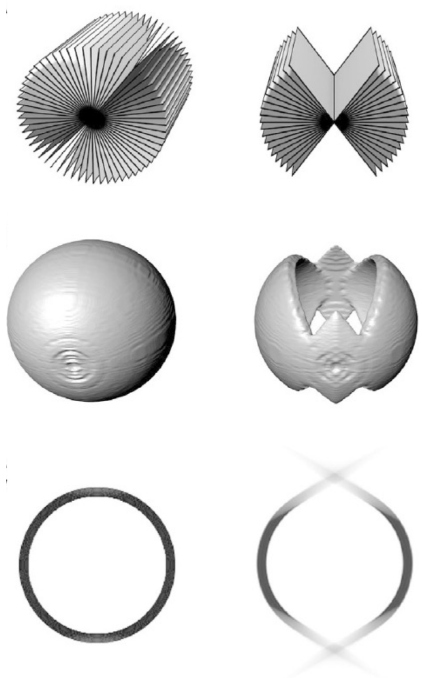

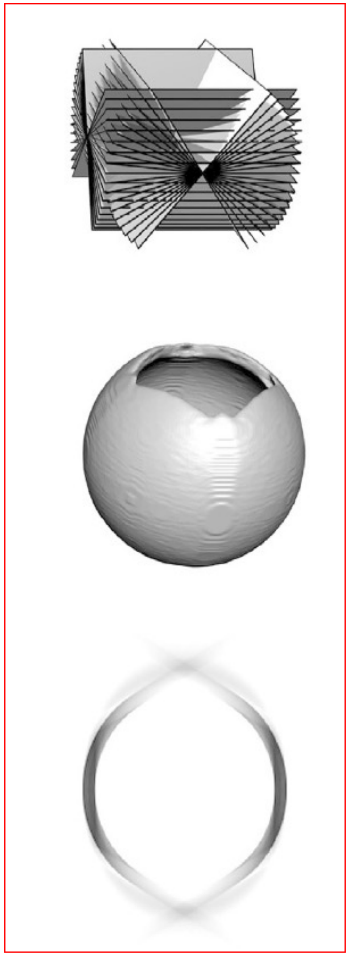

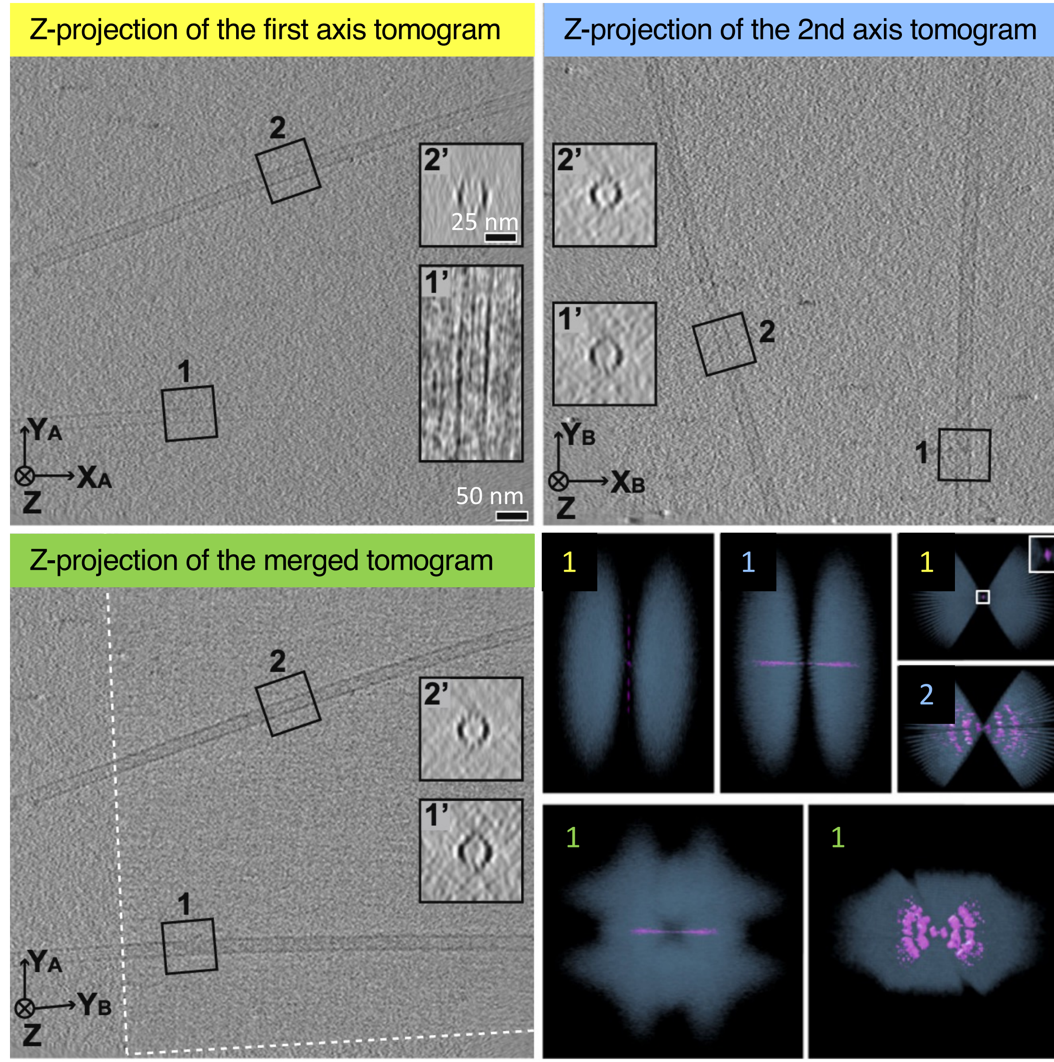

A. Guesdon et al. / Journal of Structural Biology 181 (2013) 169–178

Missing information: dual axis tomography

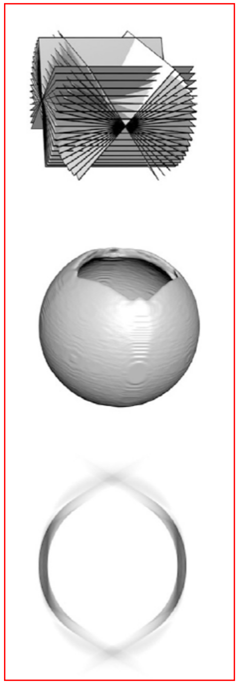

Correction of the in-plane resolution anisotropy by dual-axis cryo-electron tomography

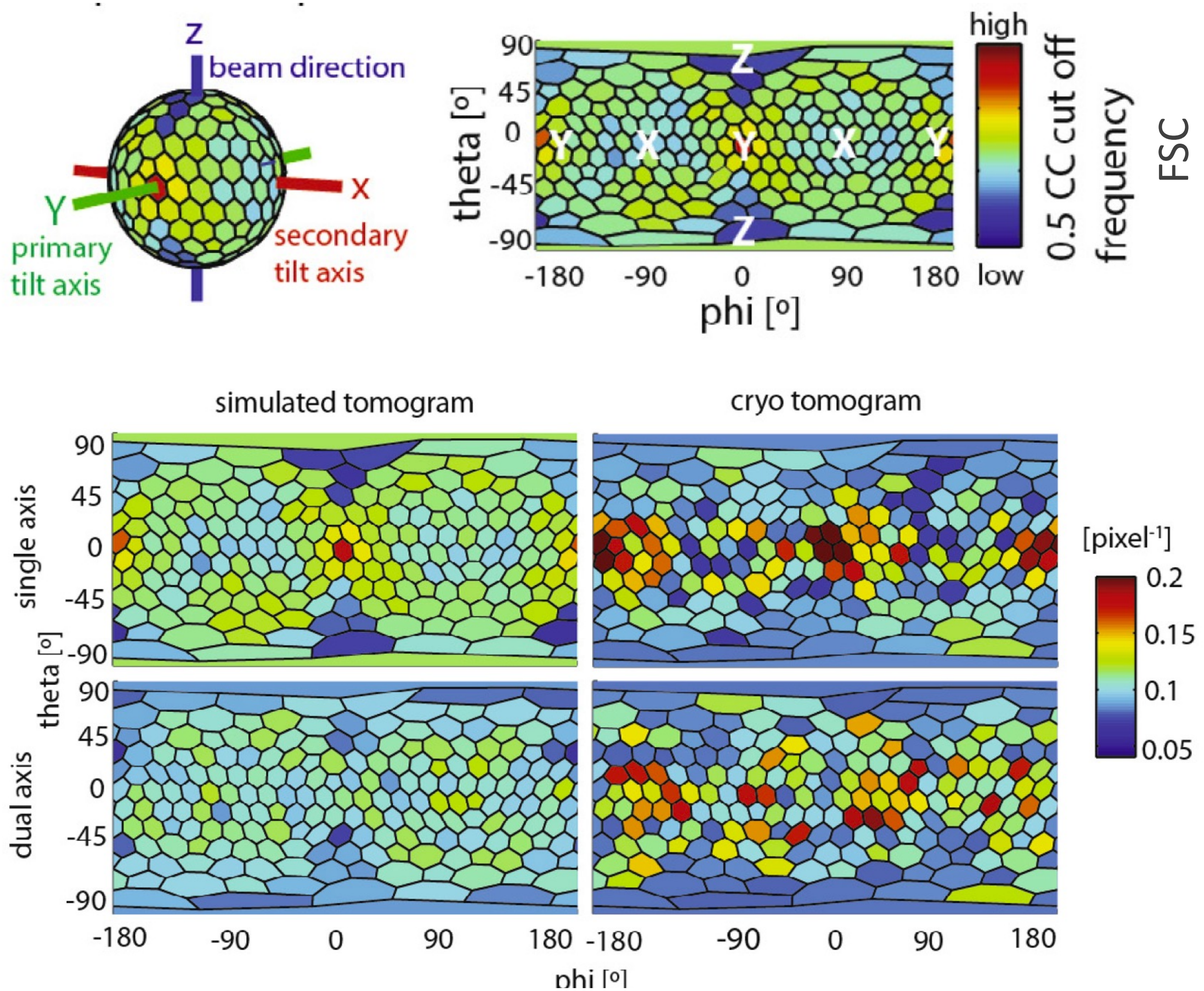

C.A. Diebolder et al. / Journal of Structural Biology 190 (2015) 215–223

Missing information: dual axis tomography

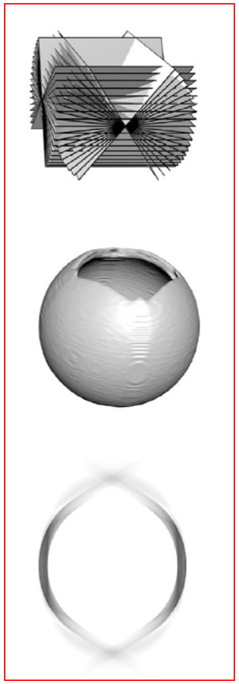

Dual axis tomography

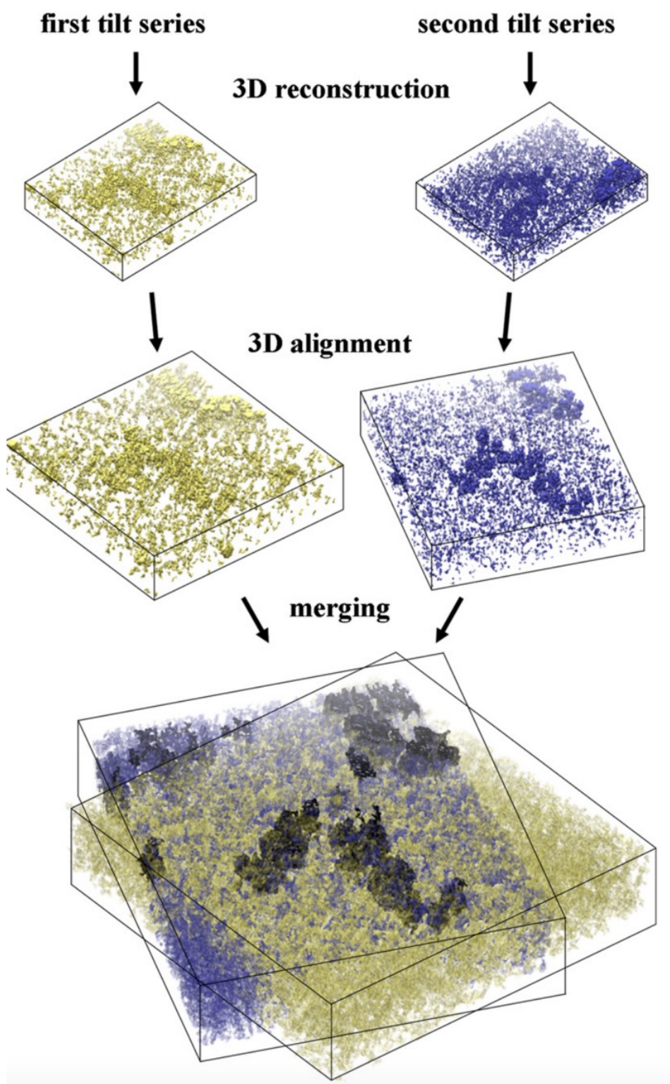

Polyribosomes

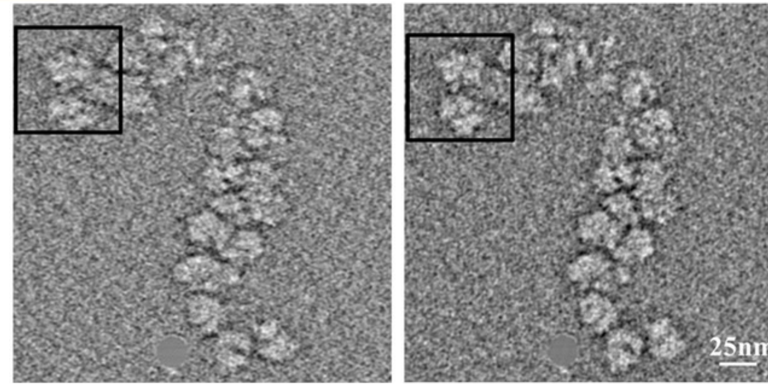

Subtomogram averaging

Dual tilt vs single tilt tomography:

- faster convergence of iterative sub-tomogram averaging
- better 3D classification using multivariate statistical analysis

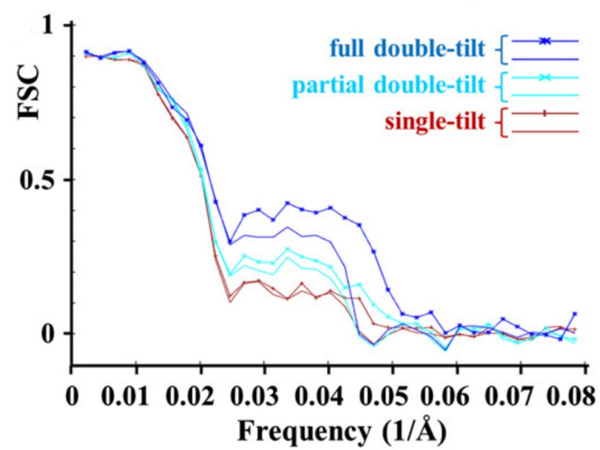

A.G. Myasnikov et al. / Ultramicroscopy 126 (2013) 33–39

Missing information: mutiple axis tomography

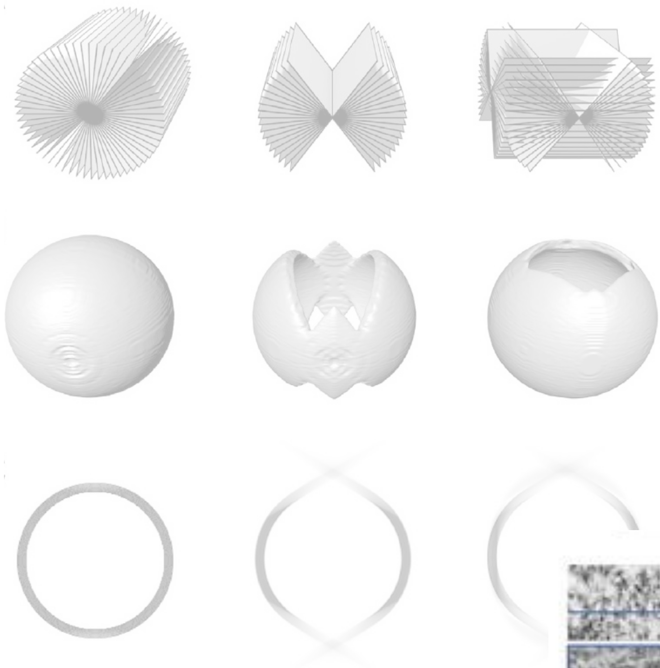

Correction of the in-plane resolution anisotropy

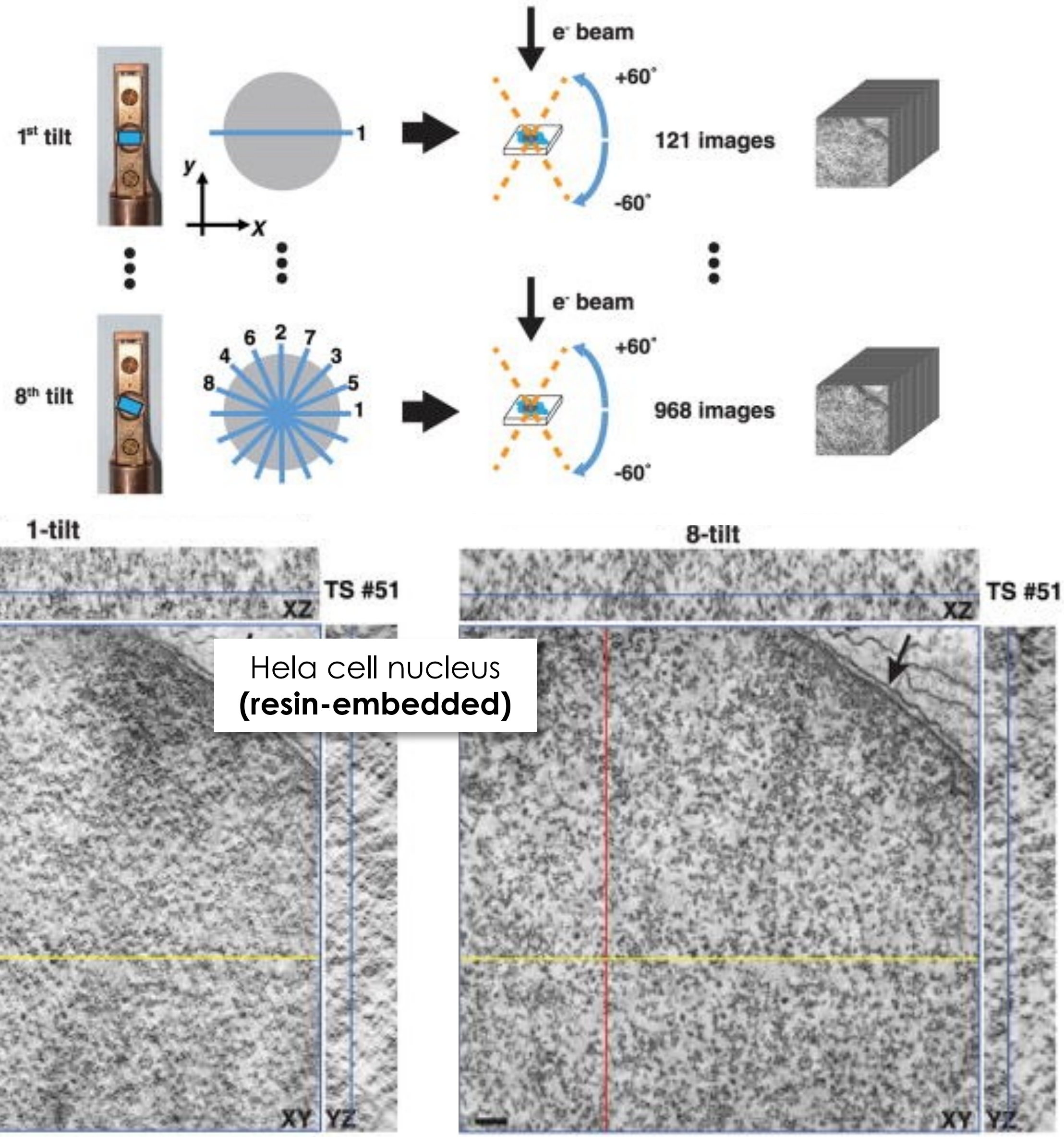

Hela cell nucleus
(resin-embedded)

Ou et al (2017) ChromEMT, *Science*

Missing information: a cylindrical holder

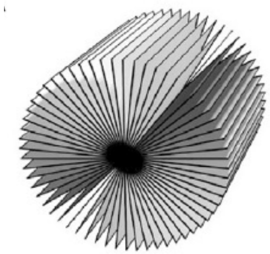

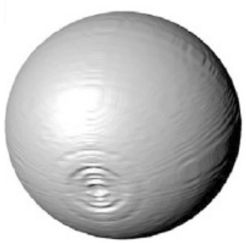

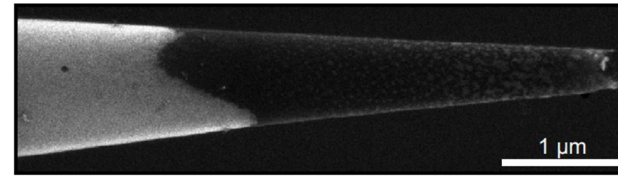

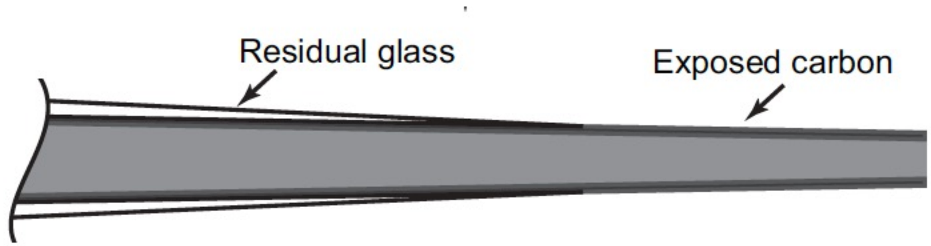

Liposomes

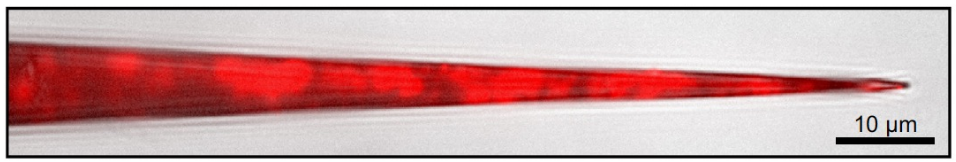

in practice
Tilt ± 73 °

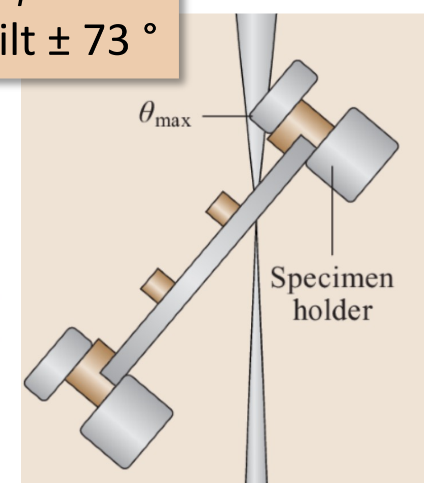

C.M. Palmer, J. Löwe / Ultramicroscopy 137 (2014) 20–29

Missing information: a cylindrical holder

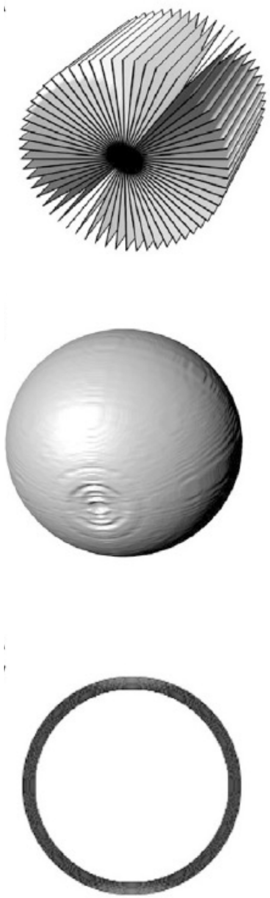

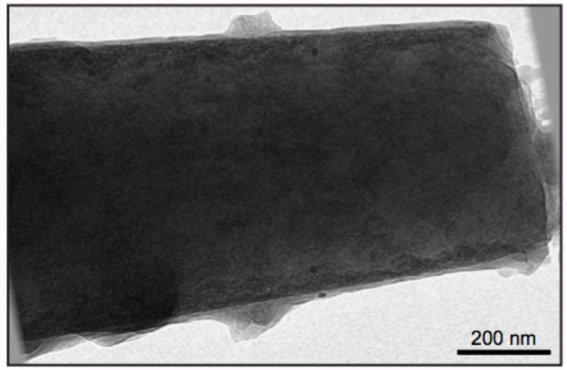

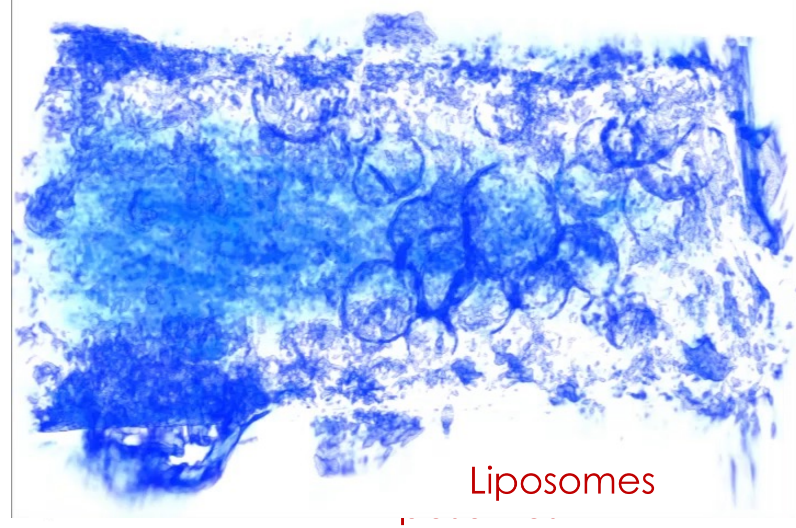

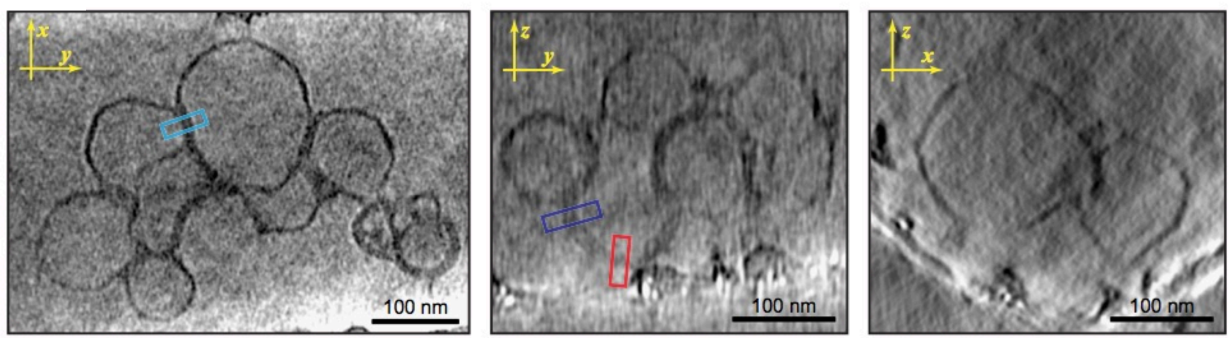

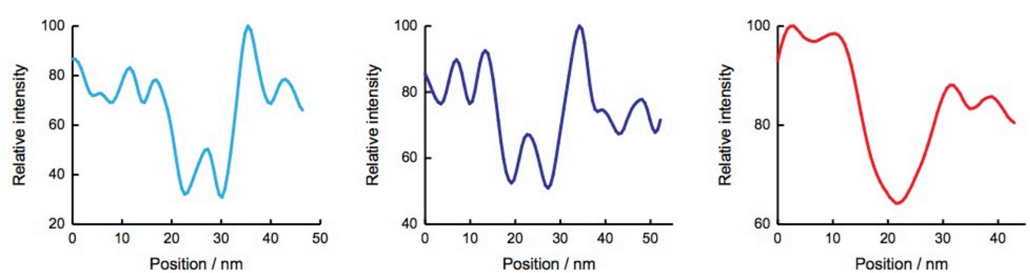

C.M. Palmer, J. Löwe / Ultramicroscopy 137 (2014) 20–29

Tilt series acquisition

- Choice of angular increment / max tilt angle
- Single axis/dual axis

- Electron dose
- Acquisition scheme

- Zero loss filtering
- Phase plates

- In practice

Tilt series acquisition: electron dose

Dose fractionation theorem

R. Hegerl & W. Hoppe (1976) Influence of Electron Noise on Three-dimensional Image Reconstruction. *Zeitschrift für Naturforschung A*. 31, 1717–1721.

Ewen et al (1995) Ultramicroscopy 60, 357-373

« the total dose required to achieve statistical significance for each voxel of a computed 3-D reconstruction is the same as that required to obtain a single 2-D image of that isolated voxel, at the same level of statistical significance. »

SPA 2D imaging 20 $e^-/Å^2$

Total electron dose

≤ 100 $e^-/Å^2$

sample
target resolution

Dose distribution

- constant
- variable with tilt angle

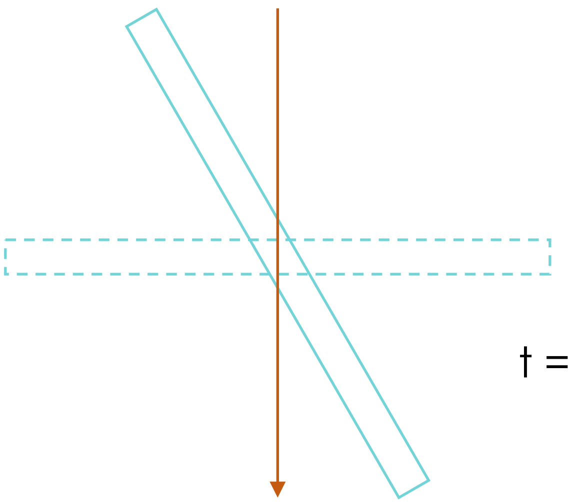

$t = t_0/\cos\theta$

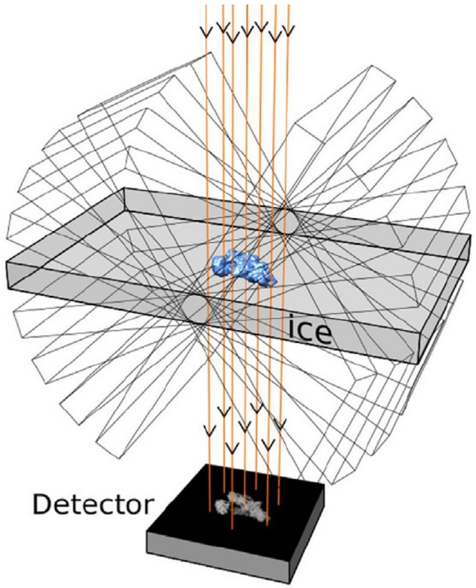

Tilt series acquisition

Acquisition schemes

Linear

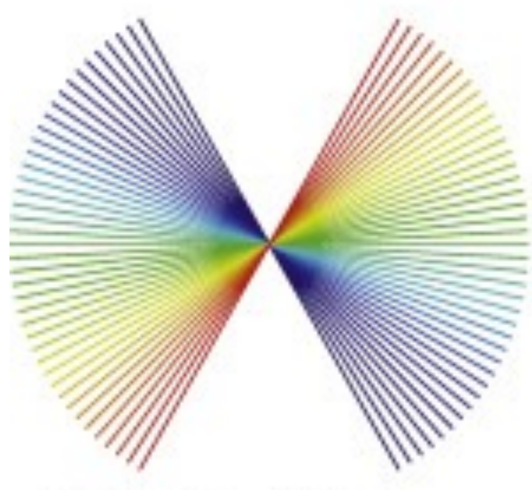

Angular increment constant

Saxton tilt scheme

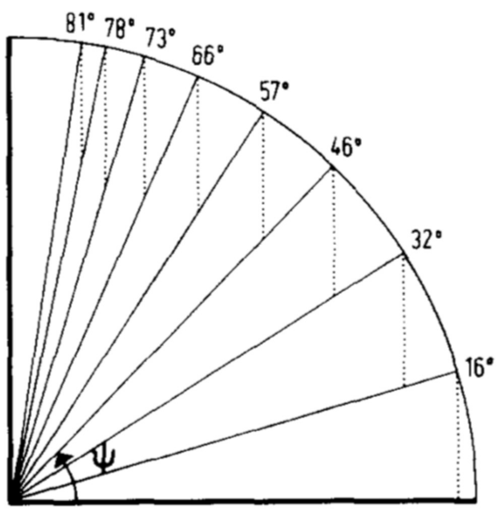

$$\alpha_{n+1} = \alpha_n + \arcsin(\sin\alpha_0 \cos\alpha_n)$$

Saxton & Baumeister, Ultramicroscopy, 1984
Grim et al, Biophys. J. 1998

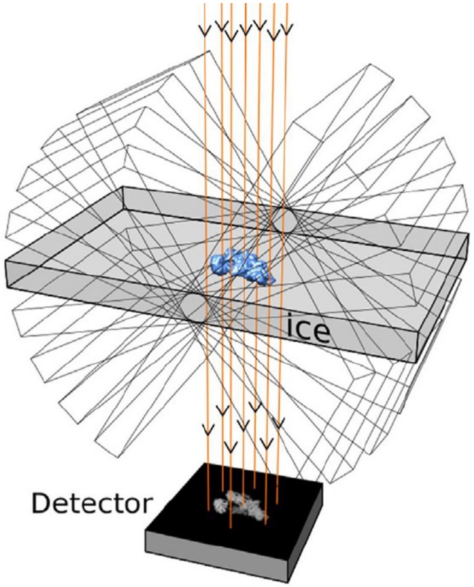

Tilt series acquisition

Acquisition schemes

Continuous | Bi-directionnal from 0 | Dose symmetric

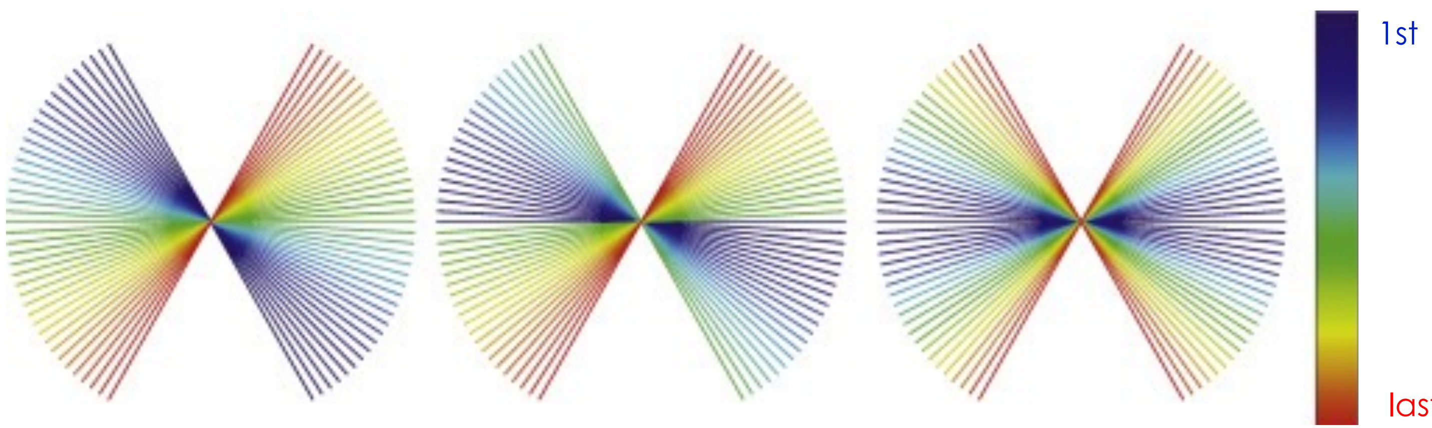

Hagen et al, J. Struct. Biol. (2017)

Zero loss filtering

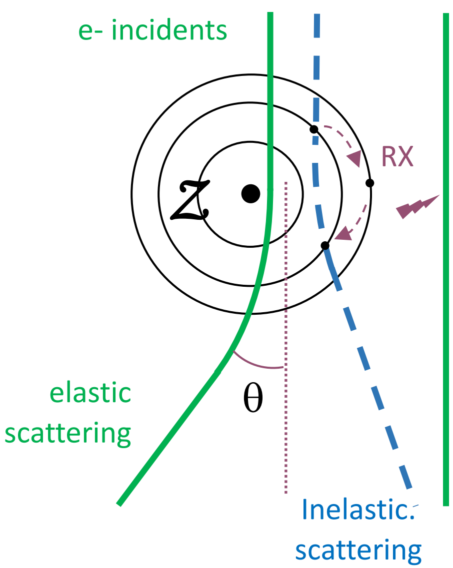

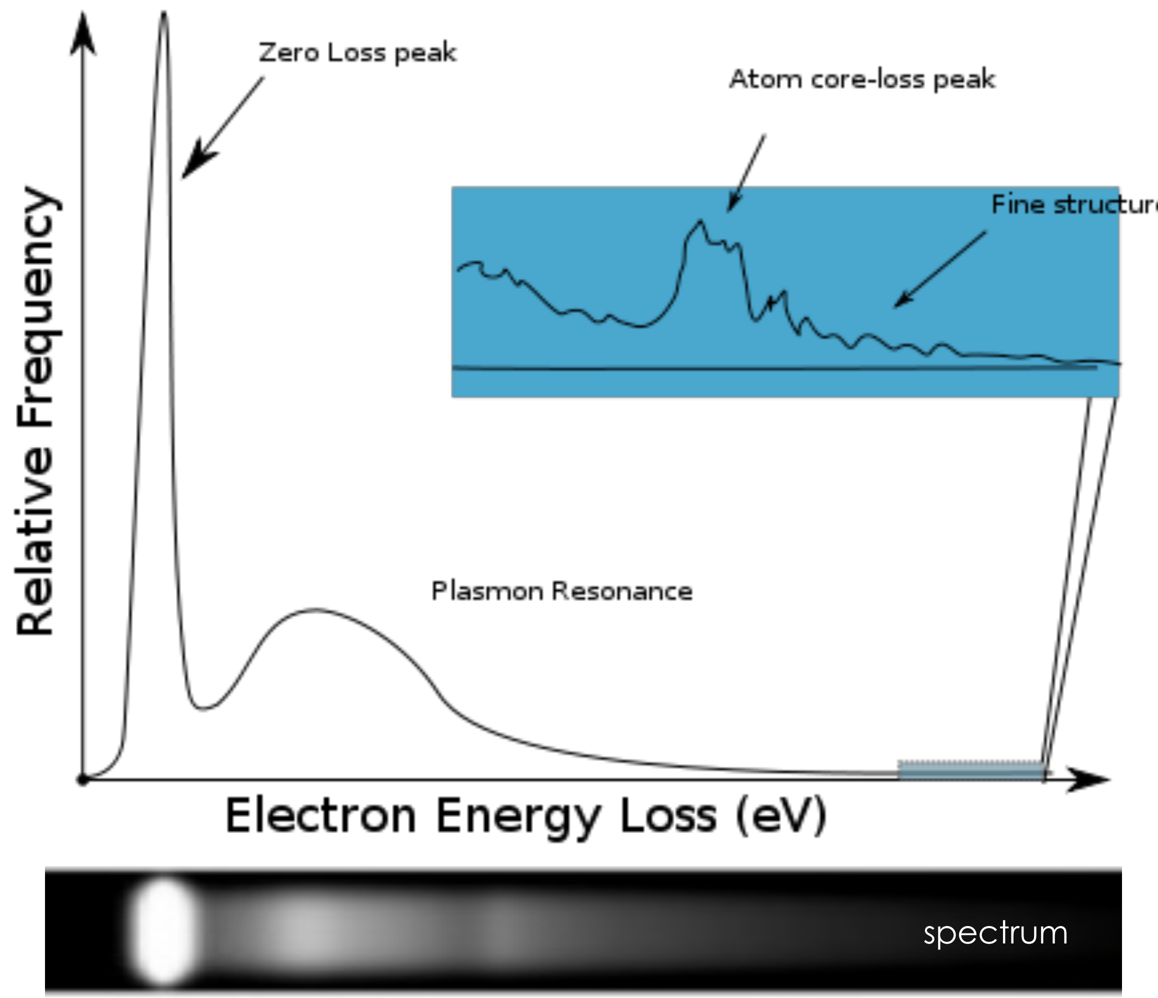

Zero loss filtering

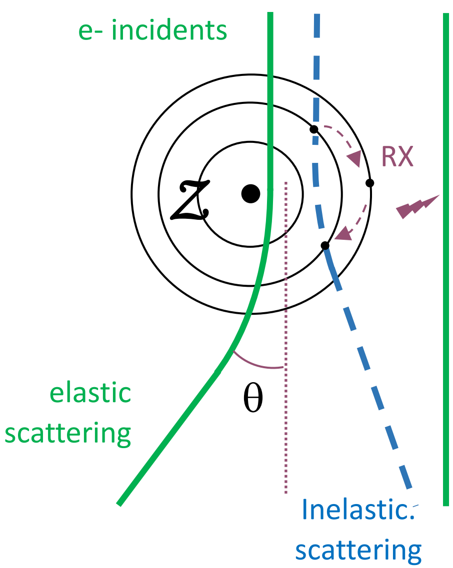

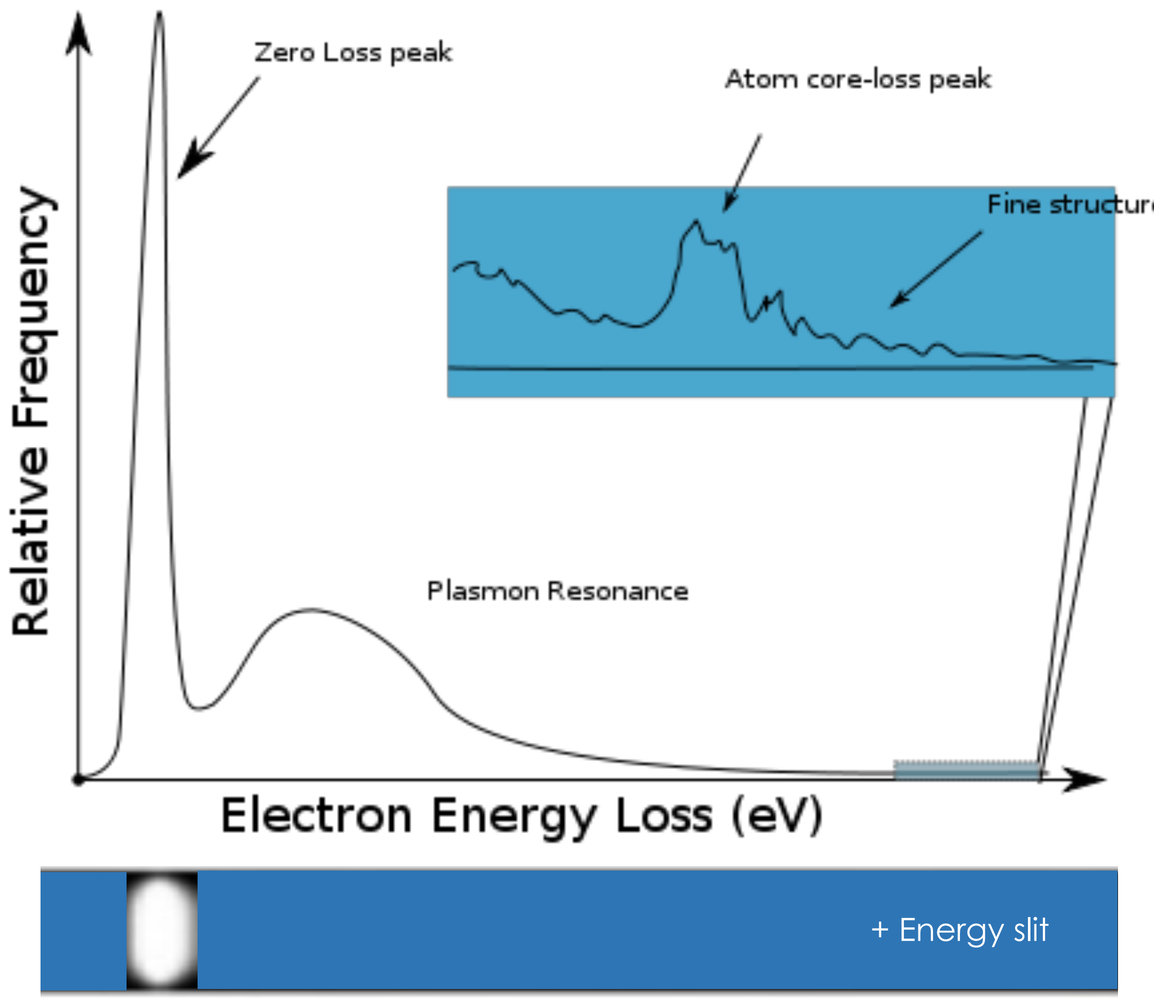

Zero loss filtering

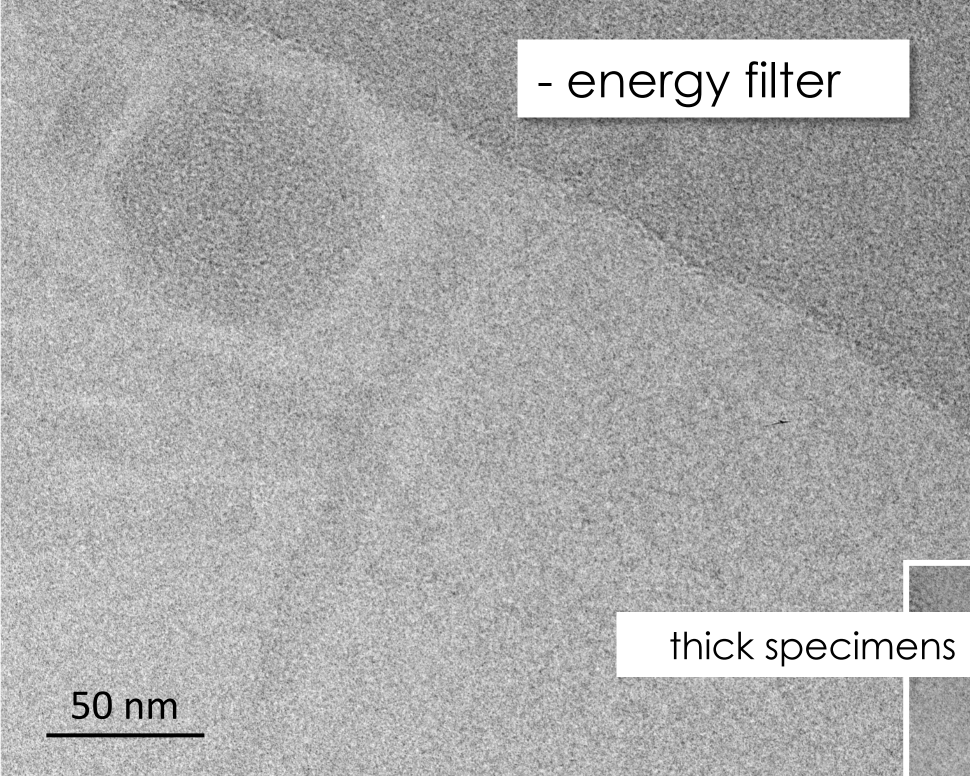

thick specimens

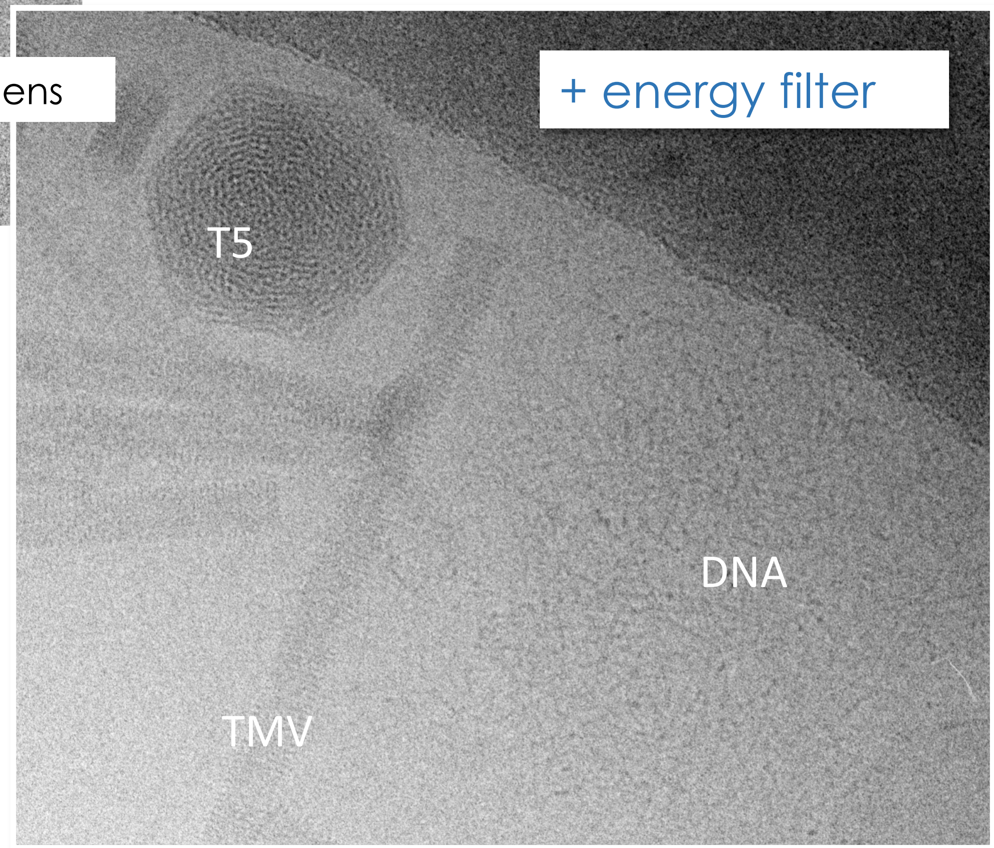

« zero loss filtering »

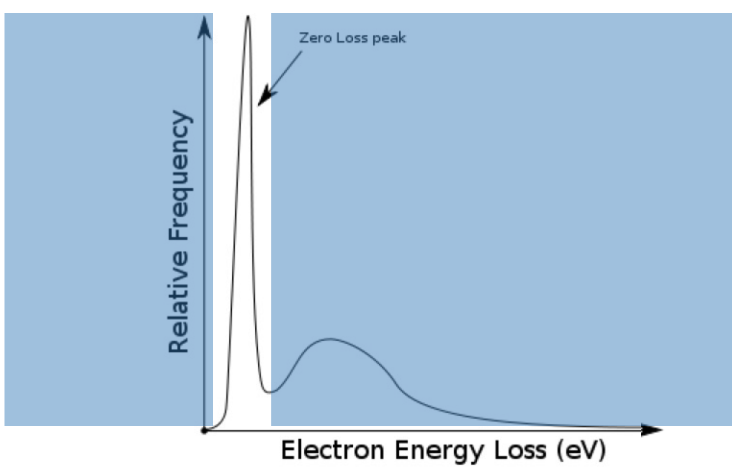

Tilt series acquisition: zero loss filtering

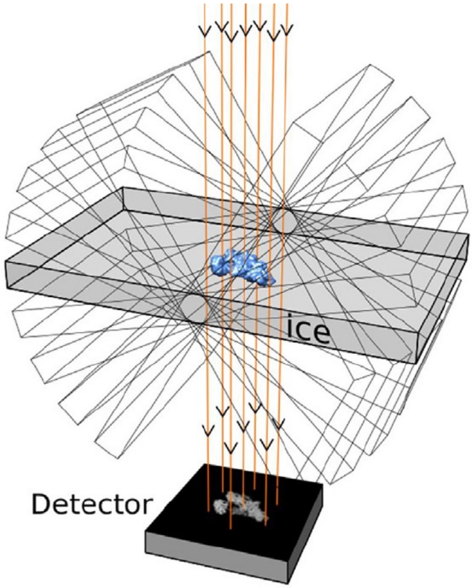

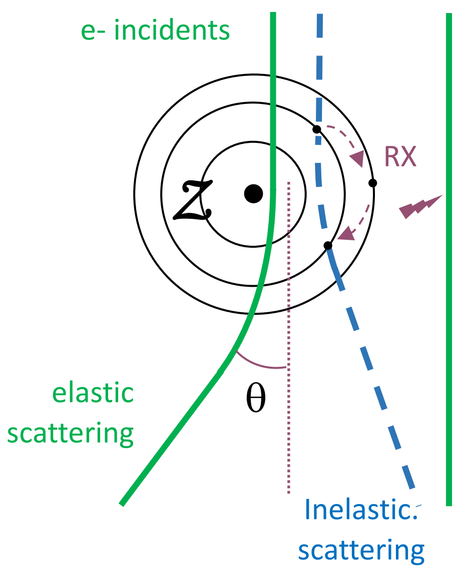

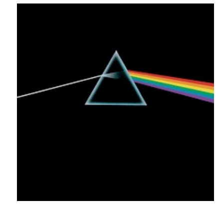

thick specimens

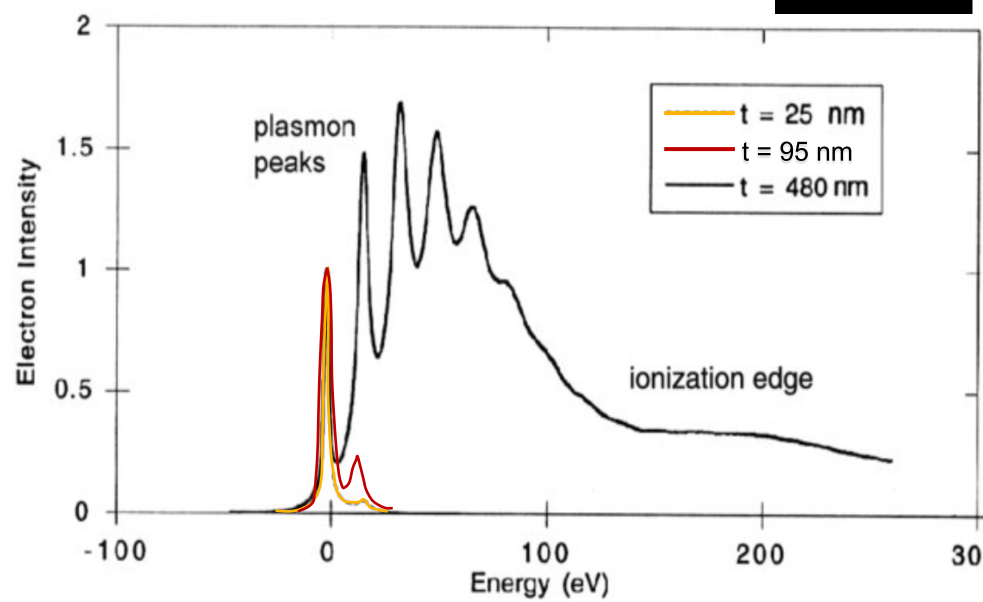

Egerton (2008) *Reports on Progress in Physics*, *72*, 016502.

Sadamatsu et al, Ultramicroscopy, 2016

Use of Phase Plates

in-focus

1.5 um defocus

Volta potential phase plate for in-focus phase contrast transmission electron microscopy

Radostin Danev, Bart Buijsse, Maryam Khoshouei, Jürgen M. Plitzko, and Wolfgang Baumeister

PNAS November 4, 2014 111 (44) 15635-15640; published ahead of print October 20, 2014 https://doi.org/10.1073/pnas.1418377111

Volta phase plate in-focus

(d)

Defocus Phase Contrast

DPC

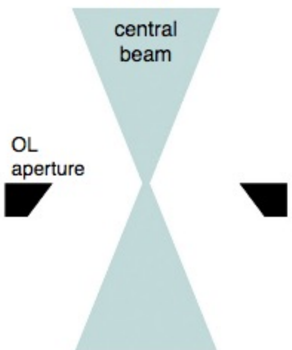

Volta potential
(beam-film interaction)

$$\boxed{\sin(\gamma(\mathbf{k}))} \rightarrow \boxed{\cos(\gamma(\mathbf{k}))}$$

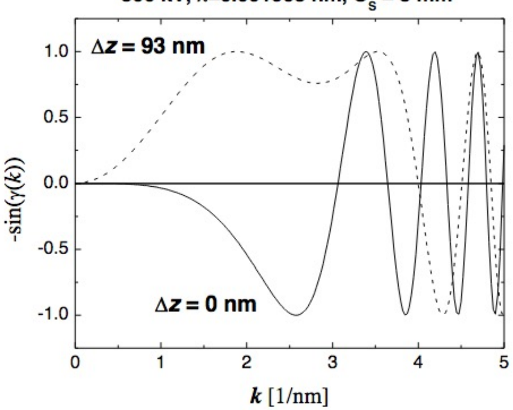

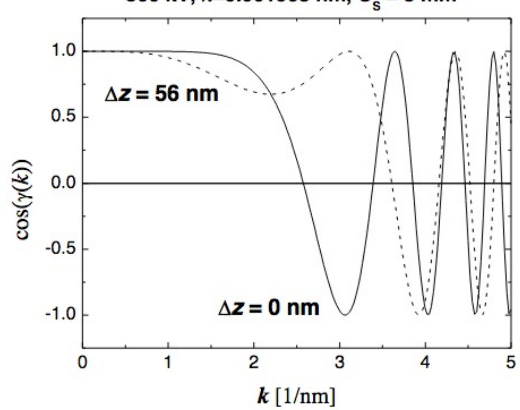

(f)

Volta Phase Plate

VPP

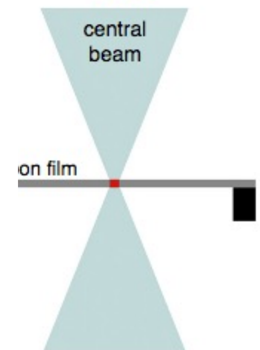

Current Opinion in Structural Biology

Use of Phase Plates

in-focus

1.5 um defocus

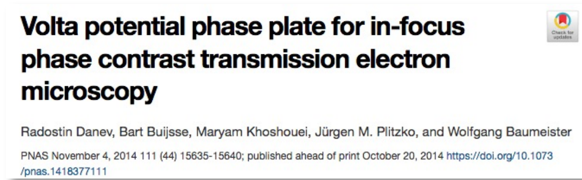
Volta potential phase plate for in-focus phase contrast transmission electron microscopy

Radostin Danev, Bart Buijsse, Maryam Khoshouei, Jürgen M. Plitzko, and Wolfgang Baumeister

PNAS November 4, 2014 111 (44) 15635-15640; published ahead of print October 20, 2014 https://doi.org/10.1073/pnas.1418377111

Volta phase plate in-focus

(d)

Defocus Phase Contrast
DPC

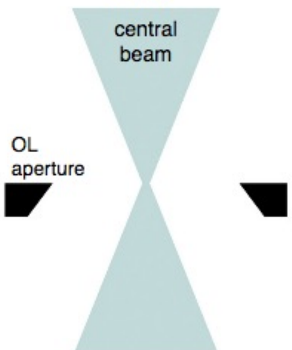

Volta potential
(beam-film interaction)

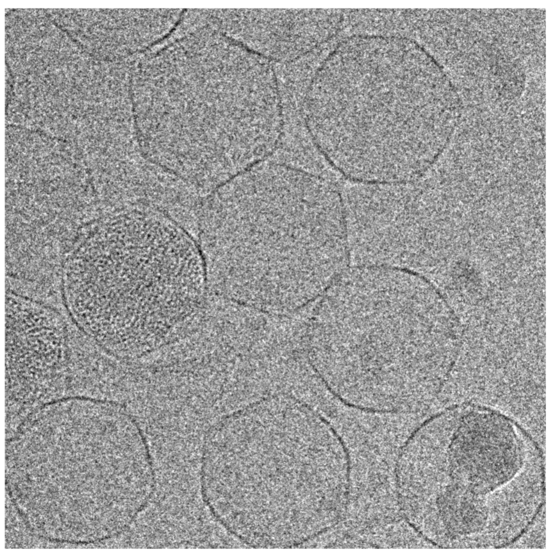

Conventional cryoEM
1 μm defocus

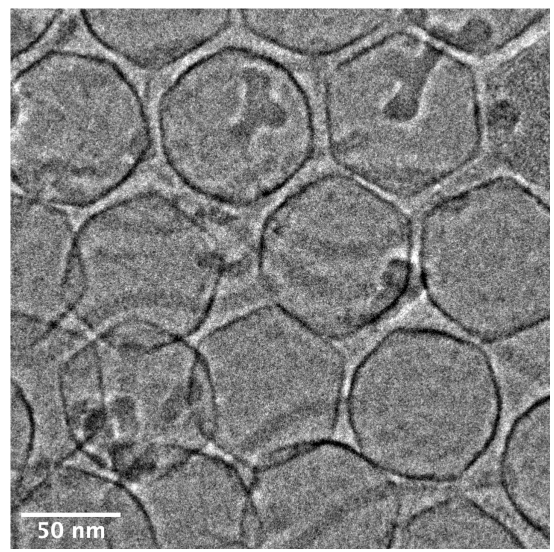

PP cryoEM
In-focus

(f)

Volta Phase Plate
VPP

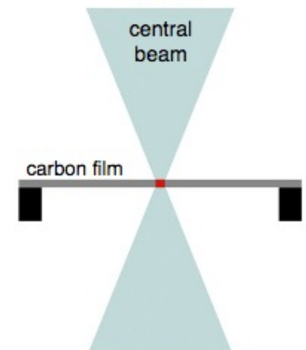

Current Opinion in Structural Biology

Tilt series acquisition: Phase Plates + energy filter

Conventional cryoEM
1μm defocus

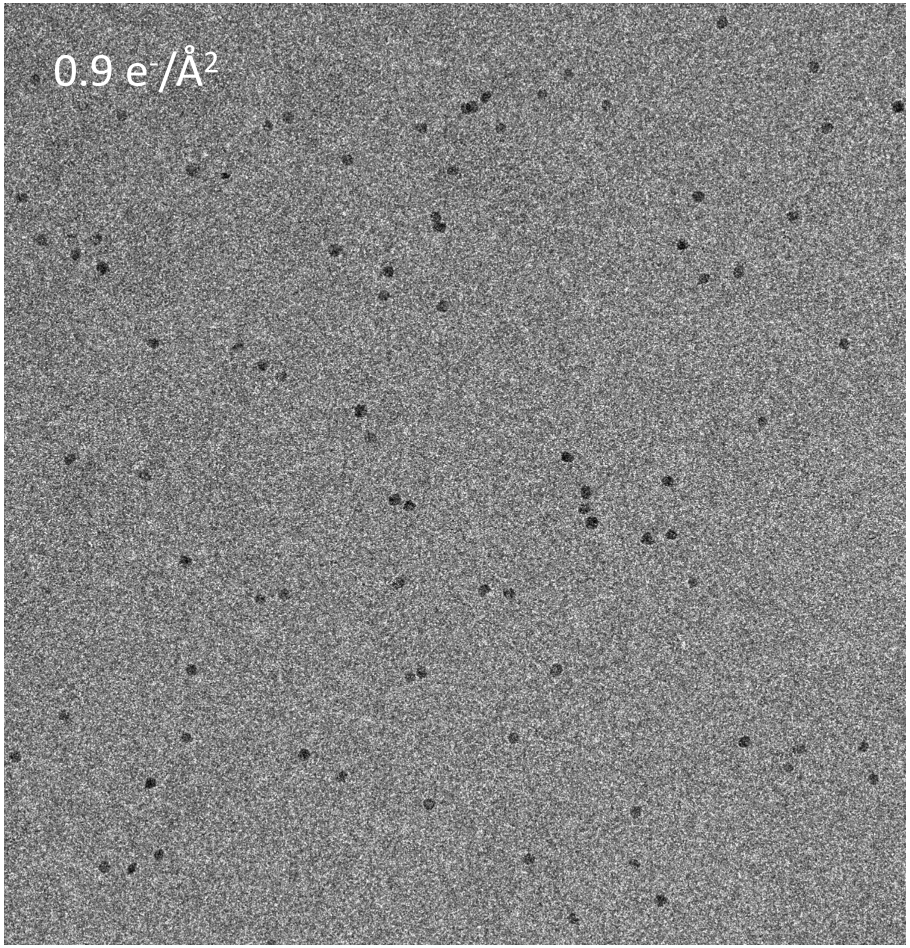

PP cryoEM
In-focus + energy filter

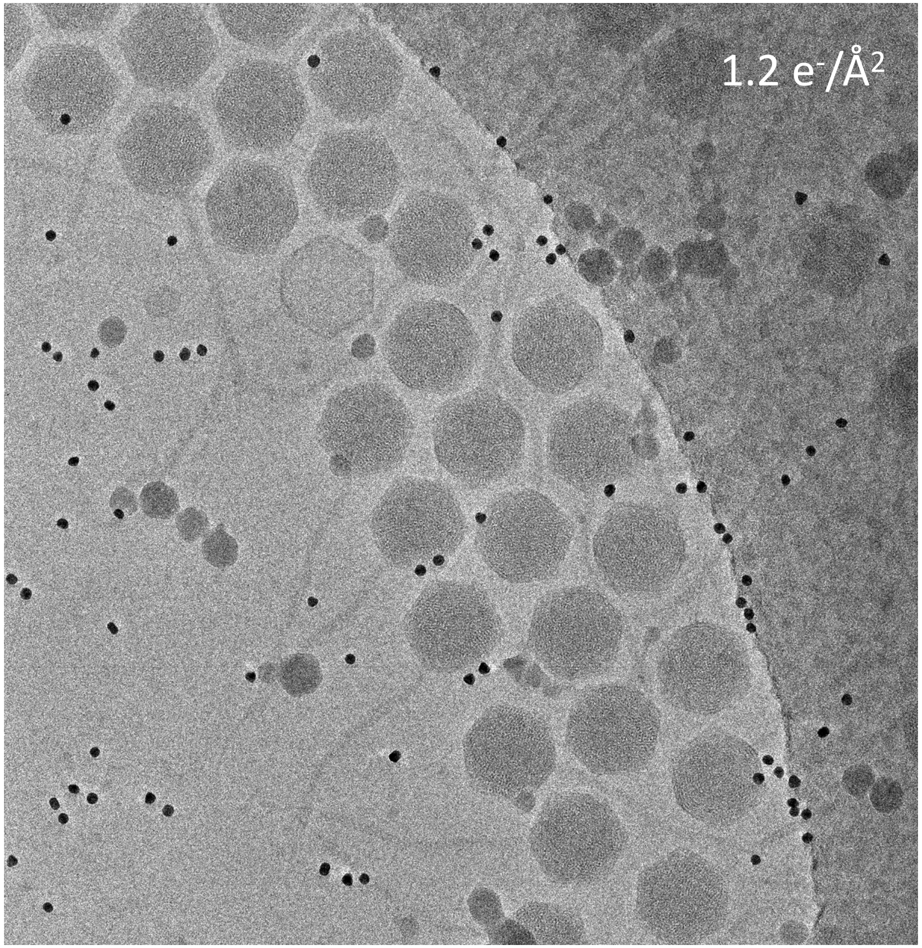

Bacteriophage T5
(80 nm) + gold NP (10 nm)

Tilt series acquisition: Phase Plates + energy filter

Conventional cryoEM
1 μm defocus

Virtual slices 0.218 nm

PP cryoEM
In-focus

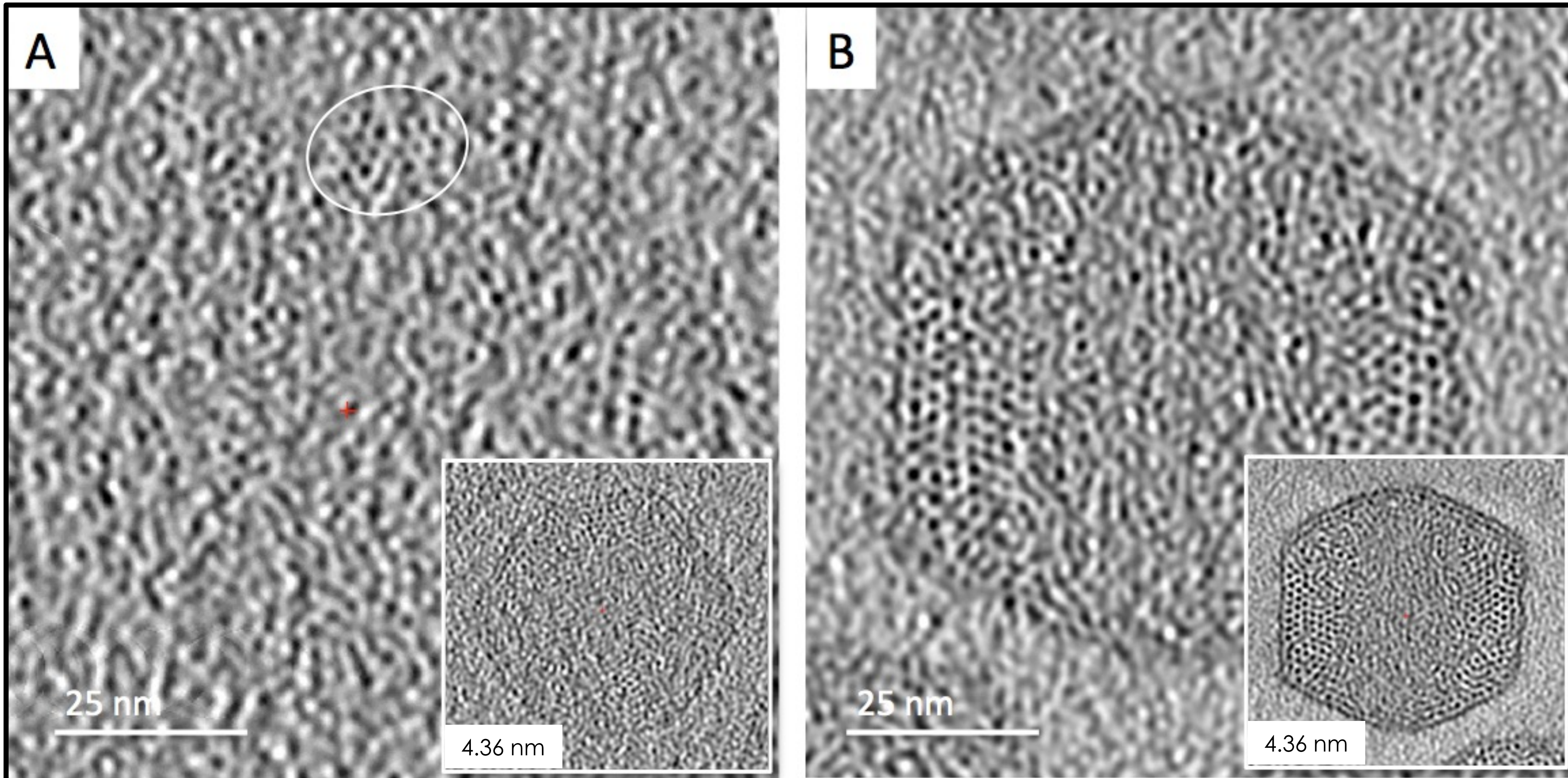

Phase Plates: limitations & perspectives

- phase shift not constant during acquisition (increases with dose accumulation)

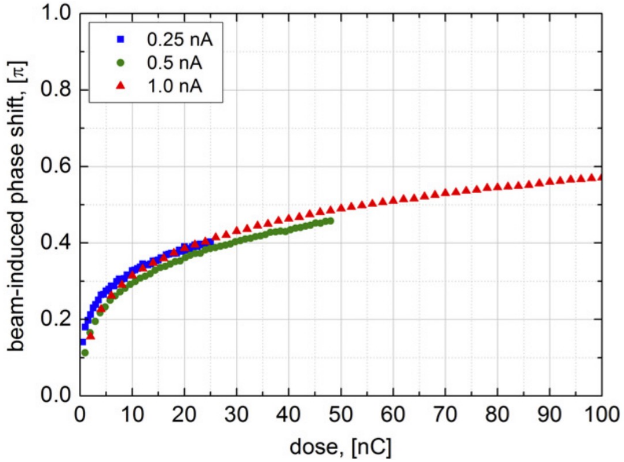

PNAS | November 4, 2014 | vol. 111 | no. 44 | 15635–15640

- signal attenuation (presence of carbon film)

- CTF determination & correction

- **tomogram segmentation**
- **sub-tomogram averaging?**

NATURE METHODS | VOL 16 | OCTOBER 2019 | 1016–1020

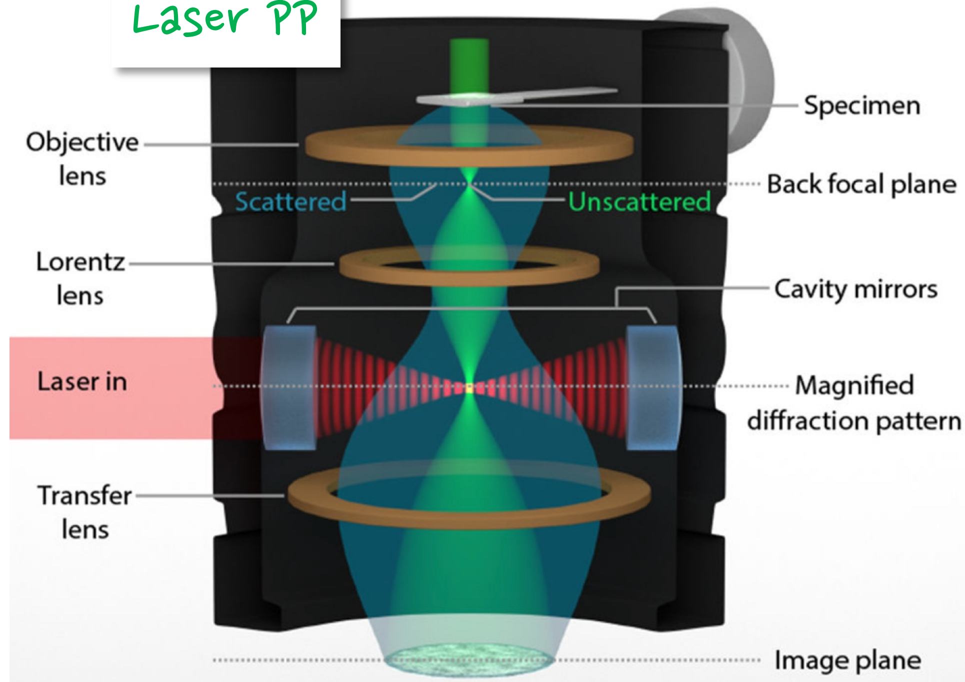

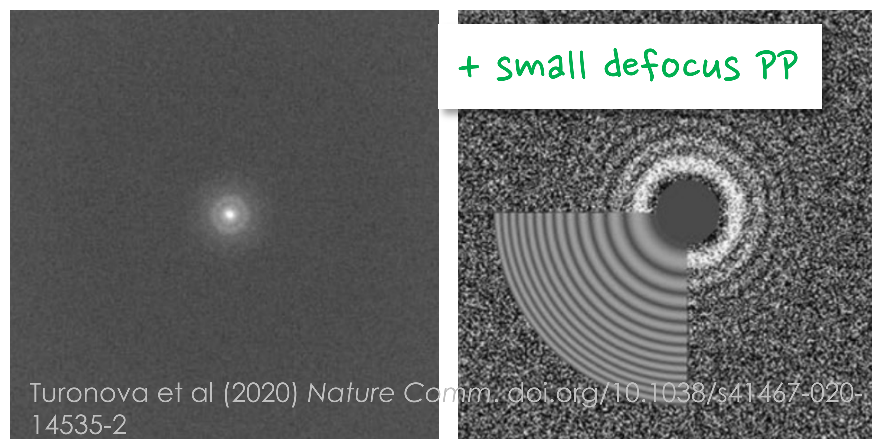

Turonova et al (2020) *Nature Comm.* doi.org/10.1038/s41467-020-14535-2

Tilt series acquisition

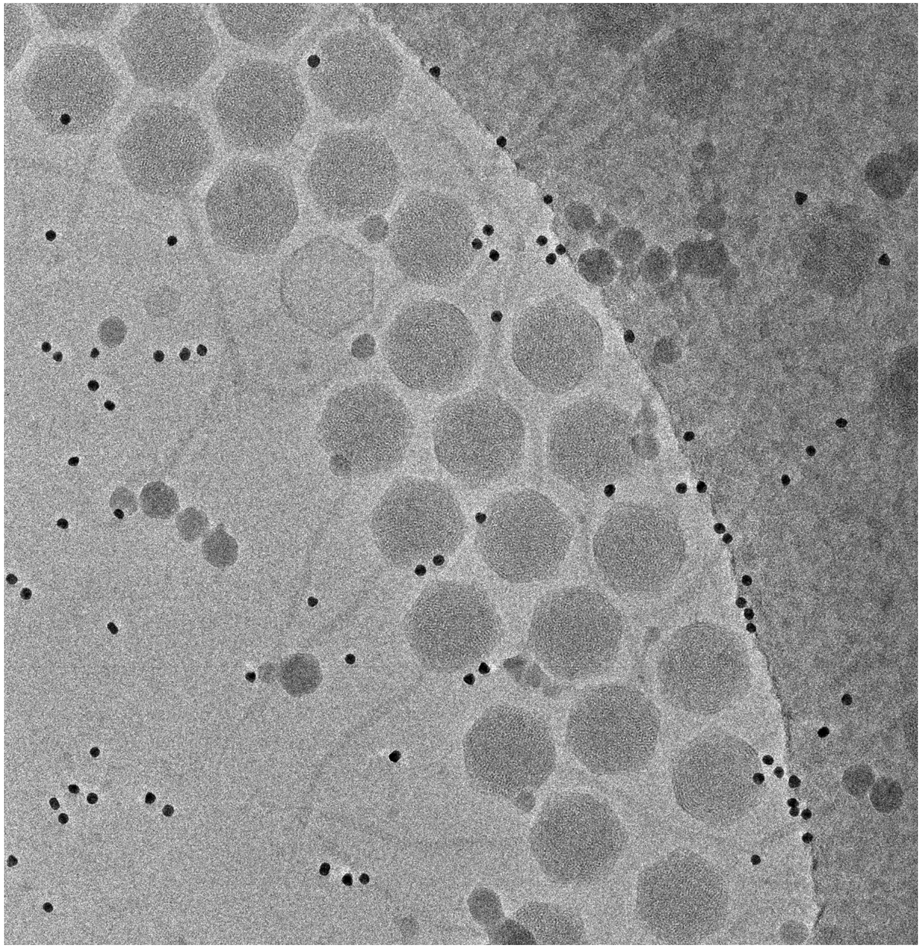

± 60°
angle increment 2°
1.2 Å² e⁻/Å²
pixel size 0.218 Å
bidirectionnal
in focus VPP
zero-loss filtering

Tilt series acquisition

tilt axis •

specimen ——

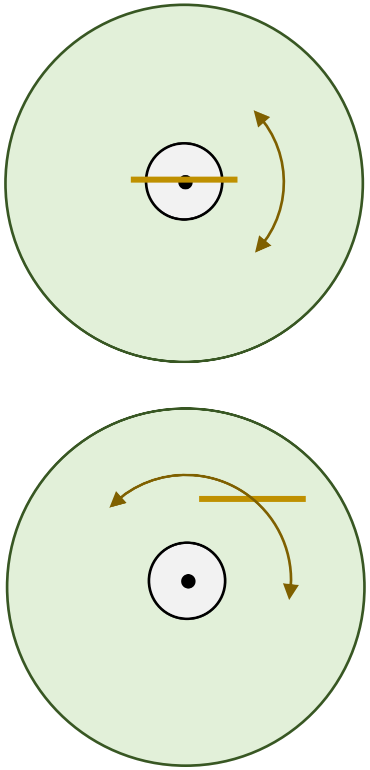

⇒ XY shifts

⇒ Z shift

(defocus, magnification)

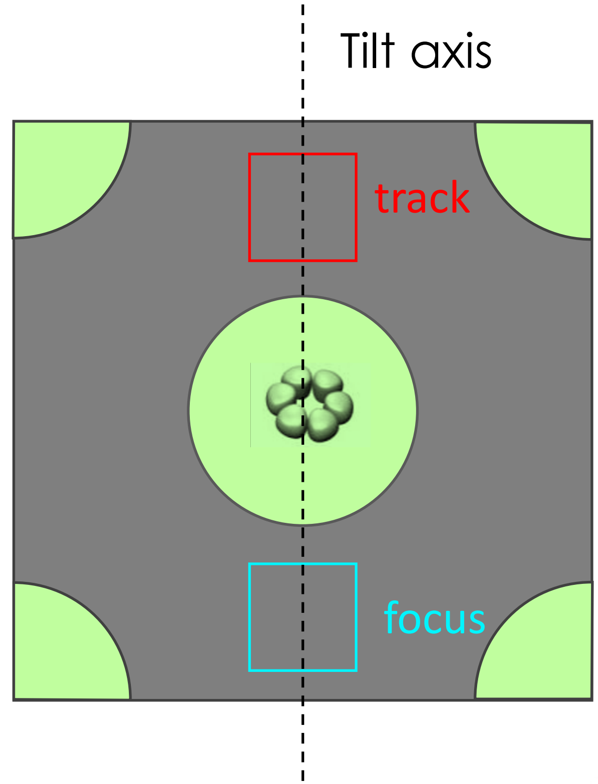

See Grant Jensen's lectures

https://www.youtube.com/playlist?list=PL8_xPU5epJdctoHdQjpfHmd_z9WvGxK8-

calibrations

Automated process

- new tilt angle
- position tracking & centering
- focus tracking & focusing
- acquisition

CTF correction

- low electron dose per image
- specimen thickness at high tilt angle
- defocus gradient

CTF correction: 2D

Correction of tilt focus gradient

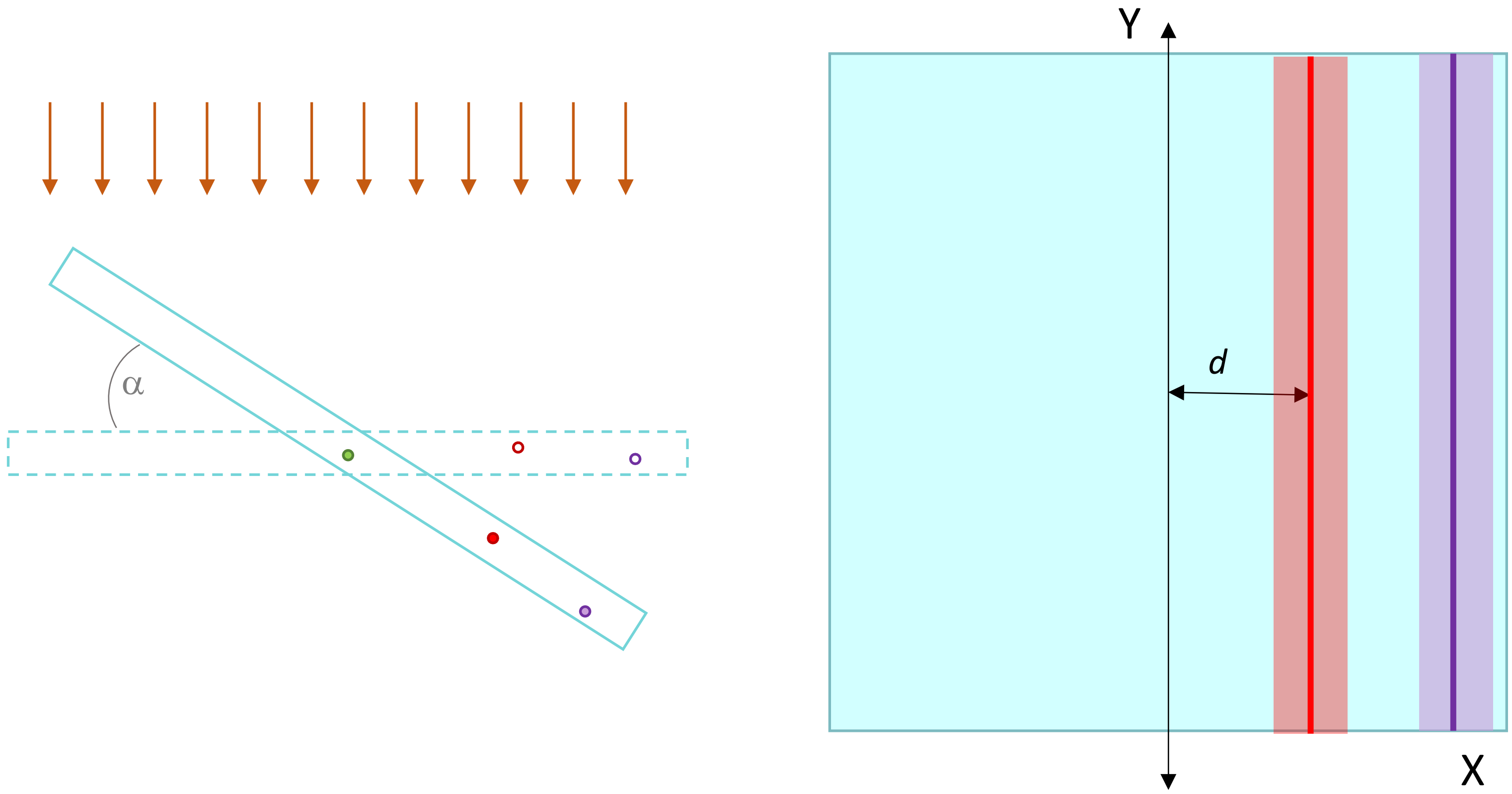

CTF correction on strips parallel to the tilt axis using the correponding local Δz values

CTF correction: 3D

Correction of the 2 focus gradients
- tilt
- thickness

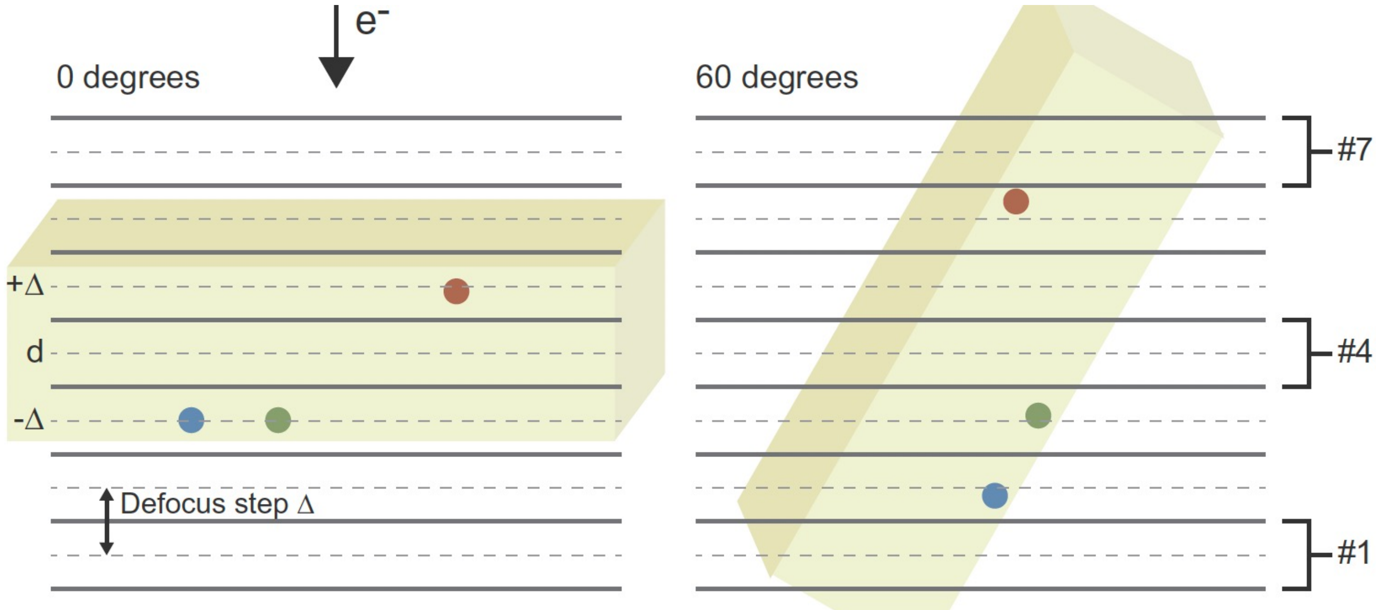

Turonova et al (2017) J. Struct. Biol. 199, 187-195

Jensen & Kornberg (2000) Ultramicroscopy, 84, 57-64

Kunz & Frangakis (2017) J. Struct. Biol. 197, 114

Turonova et al (2017) J. Struct. Biol. 199, 187-195

3D CTF correction

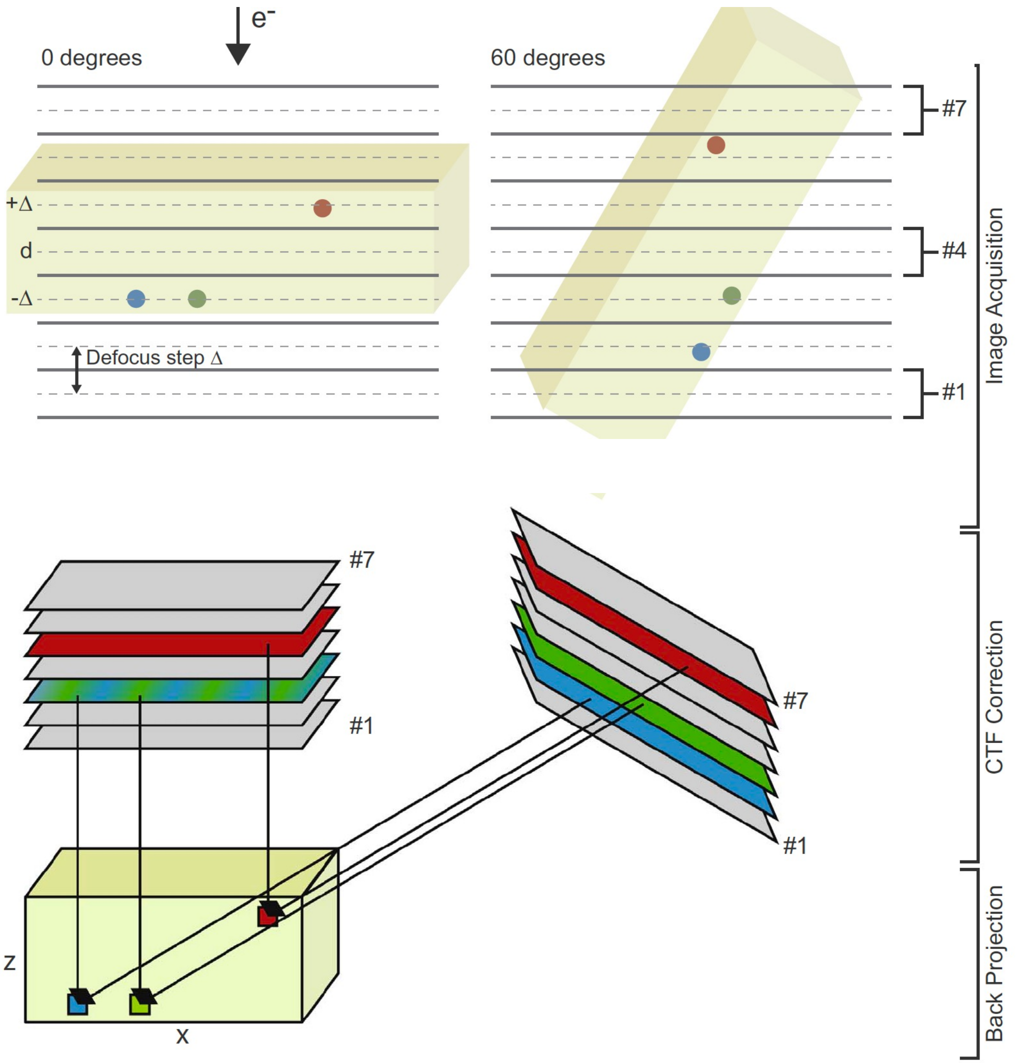

https://www.youtube.com/watch?v=8__1B2cWIFk

- division of the volume to be reconstructed into slices perpendicular to the direction of view - for each image
- each image is CTF-corrected multiple times (with different defocus value)
- back-projection of the images corrected with the appropriate defocus value

⇒ precomputed defocus array

stores value to be used for each voxel reconstruction

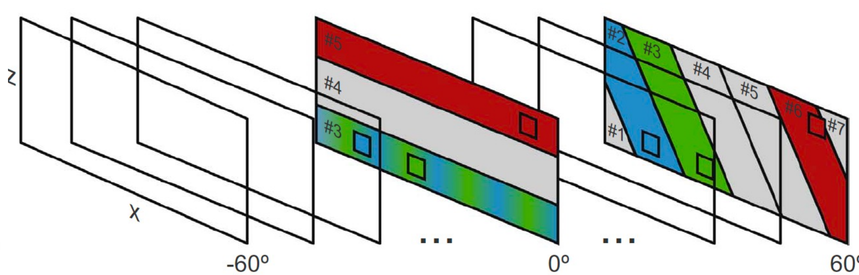

Jensen & Kornberg (2000) Ultramicroscopy, 84, 57-64 ; Turonova et al (2017) J. Struct. Biol. 199, 187-195

3D CTF correction

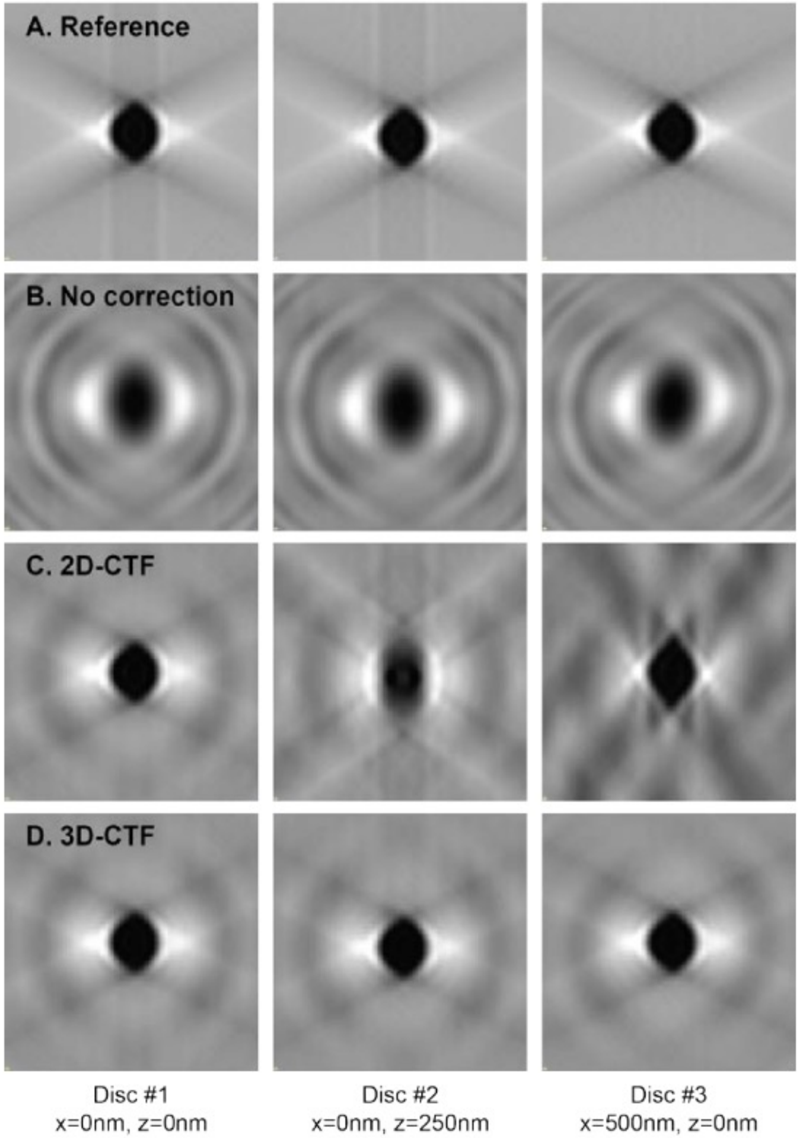

Turonova et al (2017) J. Struct. Biol. 199, 187-195

3D CTF correction

CTF model using defocus estimates for each particle in all images of the tilt series

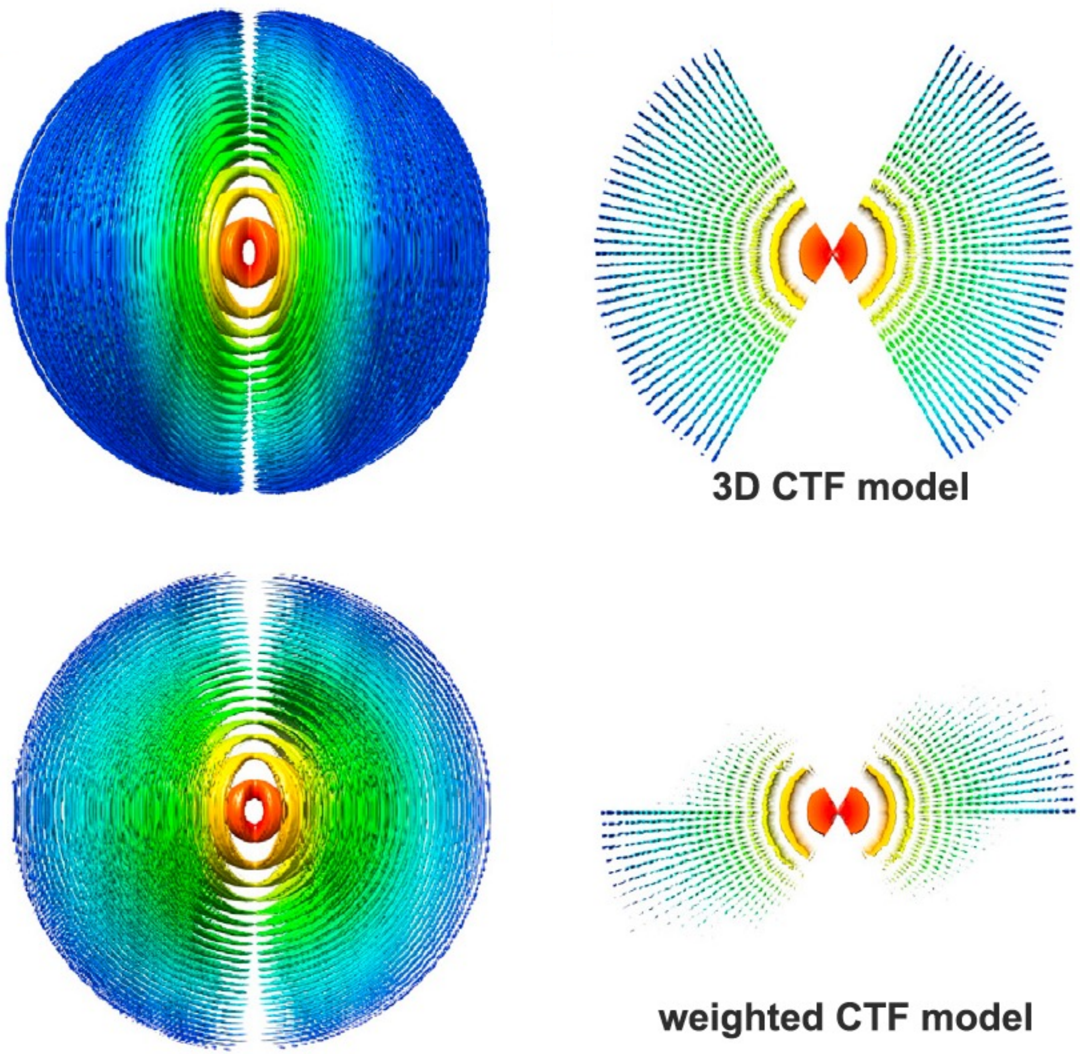

Weighted:
with electron dose
with tilt angle

Bharat et al., 2015, Structure 23, 1743–1753

Tomogram reconstruction

- Image alignment
- Reconstruction: WBP, iterative methods
- Tomogram visualisation

Image alignment

Objective: determine and correct the shift, scale, in-plane rotation and tilt angle

Coarse alignment (cross-correlation)

- Tracking of high contrast fiducial markers: gold nanoparticles (10 nm)

Detect fiducial markers (manual/automatic)

- Fiducial less alignment

“patch tracking” methods
correlation-based, possibly iterative

Generation of fiducial (patch) projection model

Image alignment

Bacteriophage T5 (80 nm)
+ gold NP (10 nm)

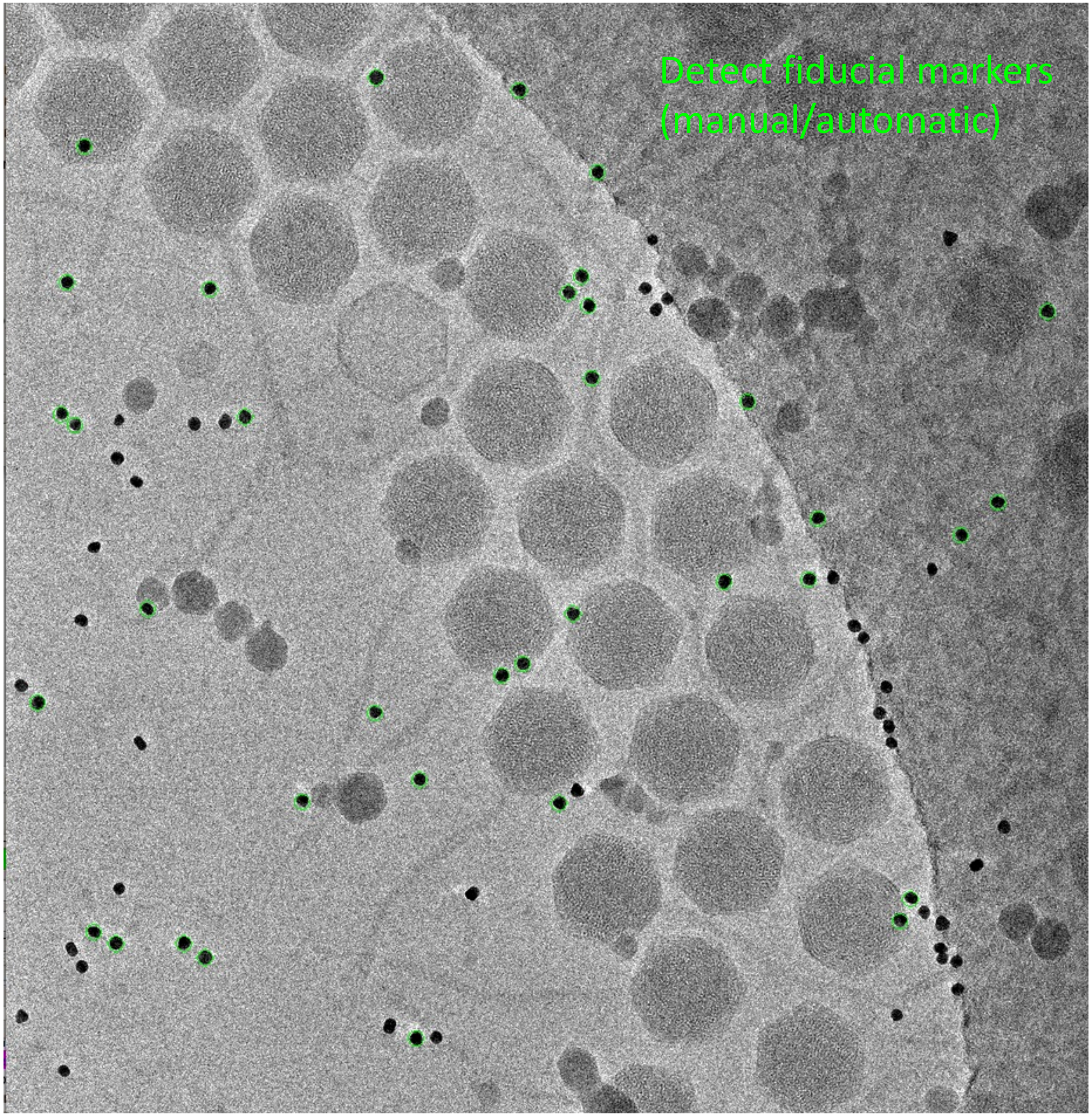

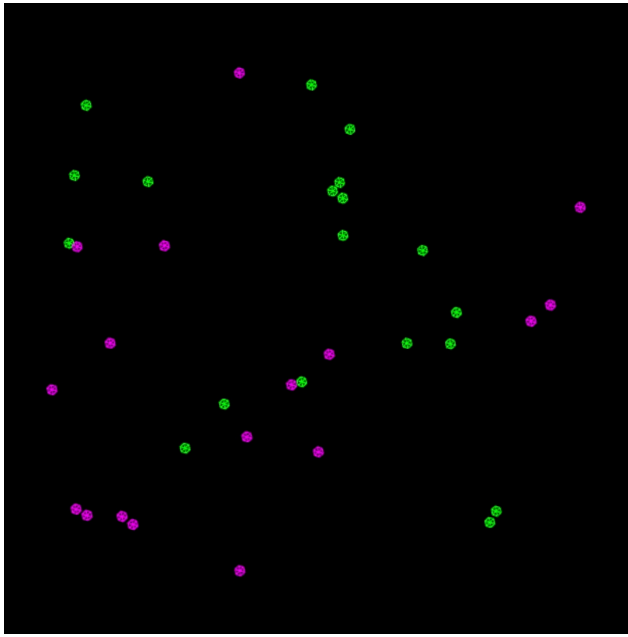

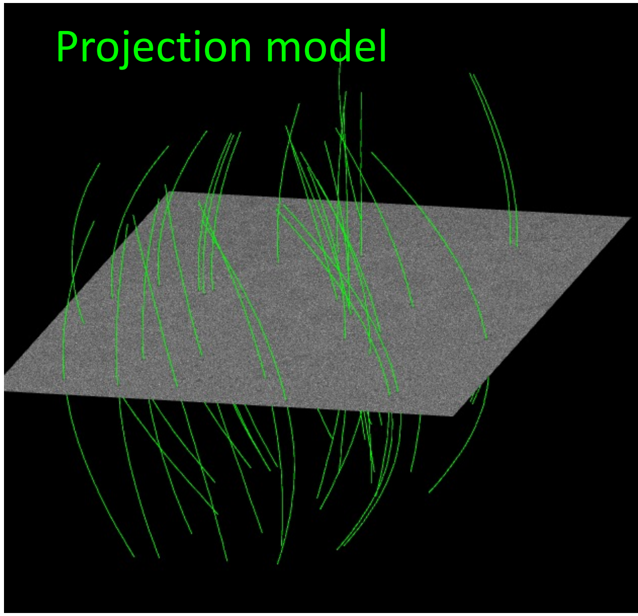

Image alignment: patch tracking methods

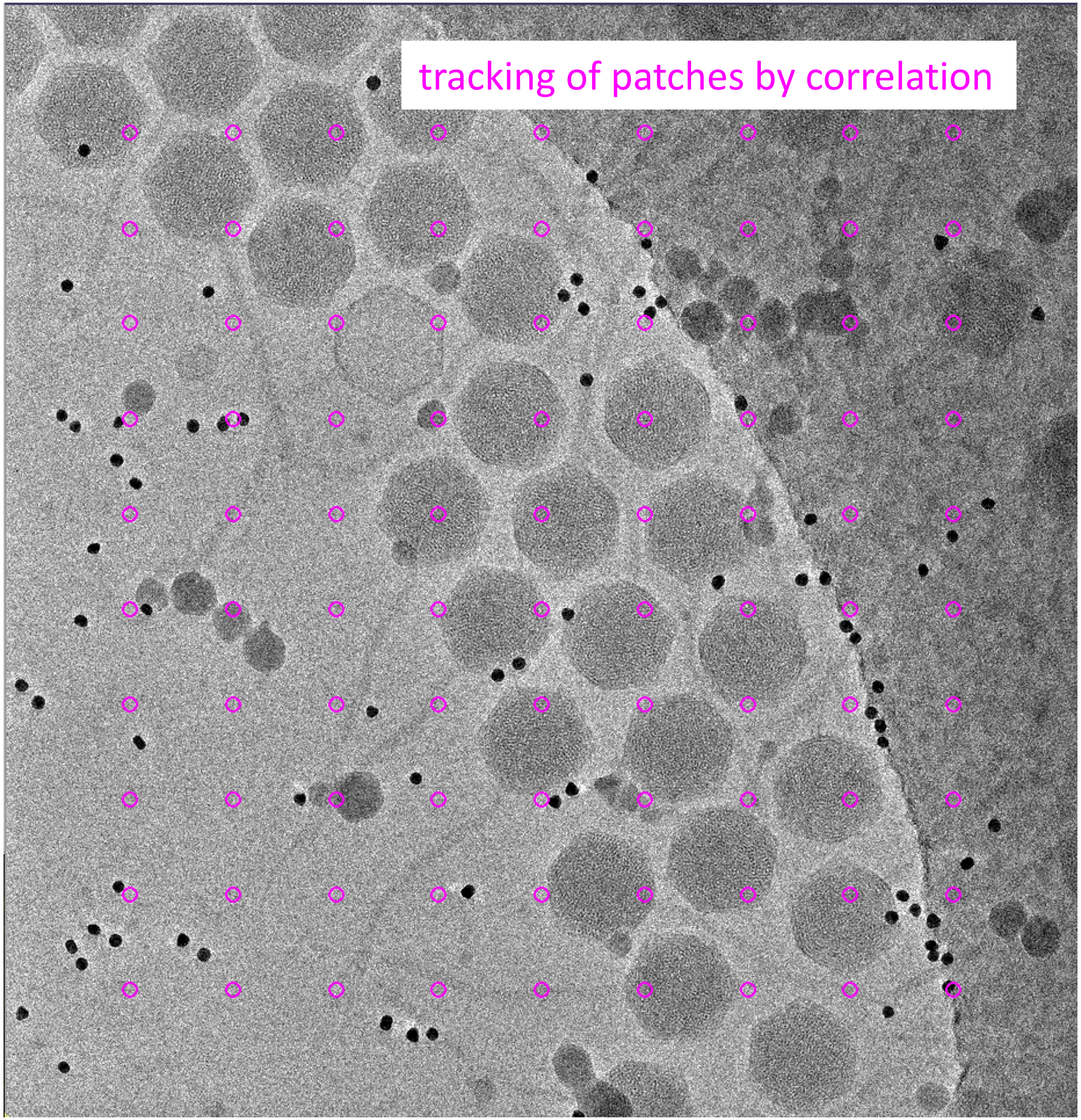

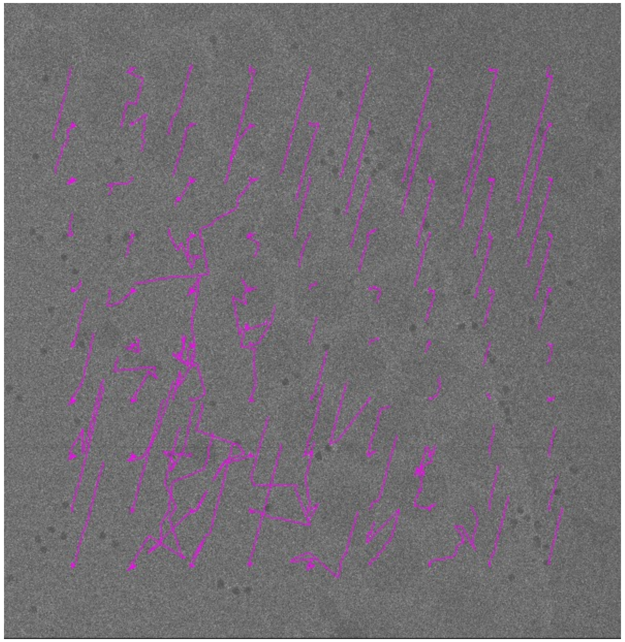

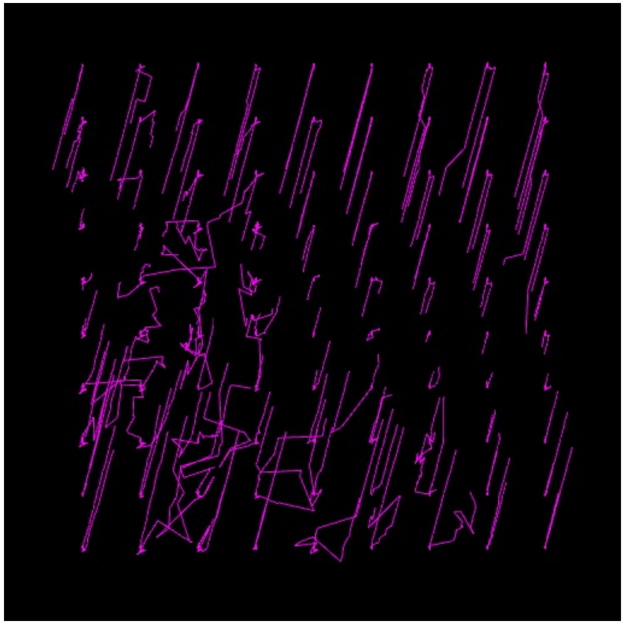

Image alignment: patch tracking methods

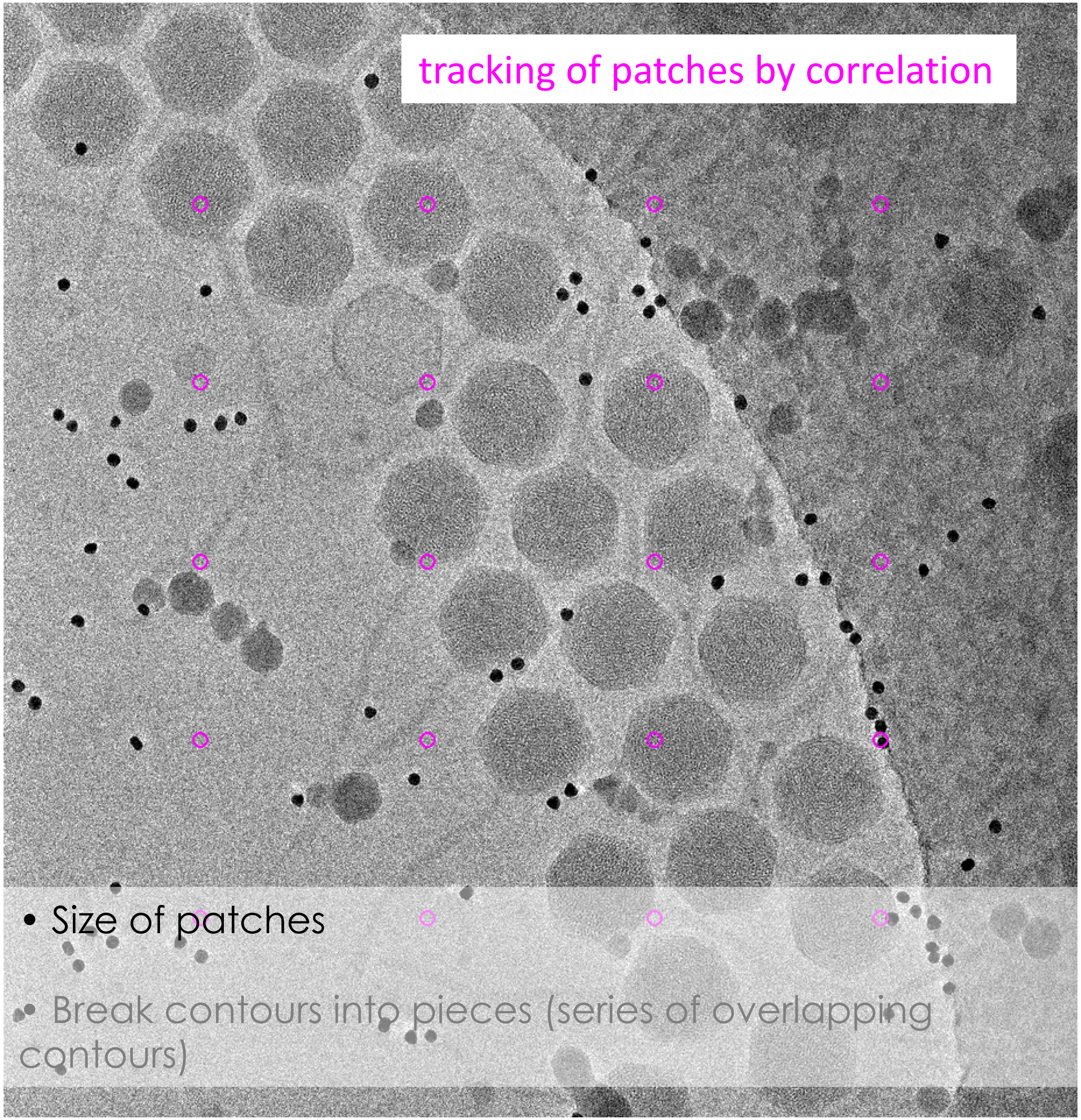

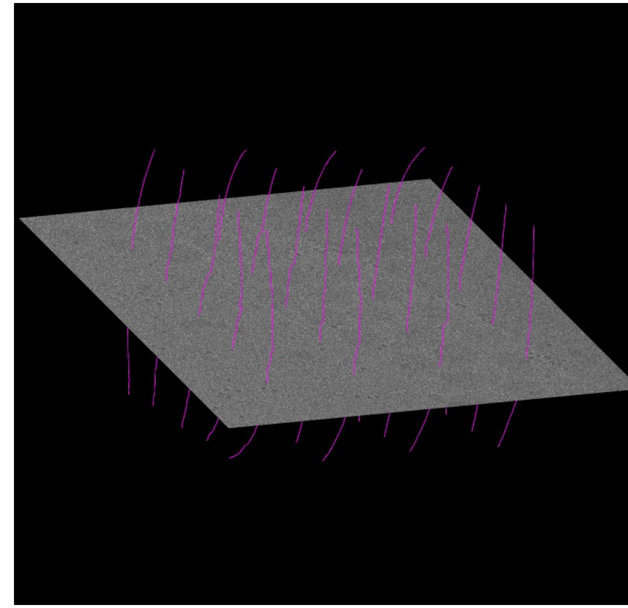

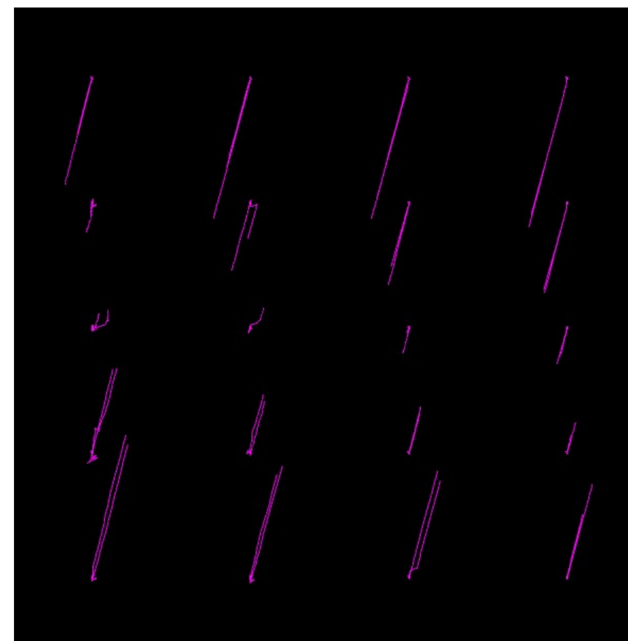

- Size of patches
- Break contours into pieces (series of overlapping contours)

Image alignment

Objective: determine and correct the shift, scale, in-plane rotation and tilt angle

Coarse alignment (cross-correlation)

- Tracking of high contrast fiducial markers: gold nanoparticles (10 nm)

Detect fiducial markers (manual/automatic)

- Fiducial less alignment

"patch tracking" methods
correlation-based, possibly iterative

Generation of fiducial (patch) projection model

Trajectory prediction & difference minimization

⇒ **Image alignment**

Image alignment

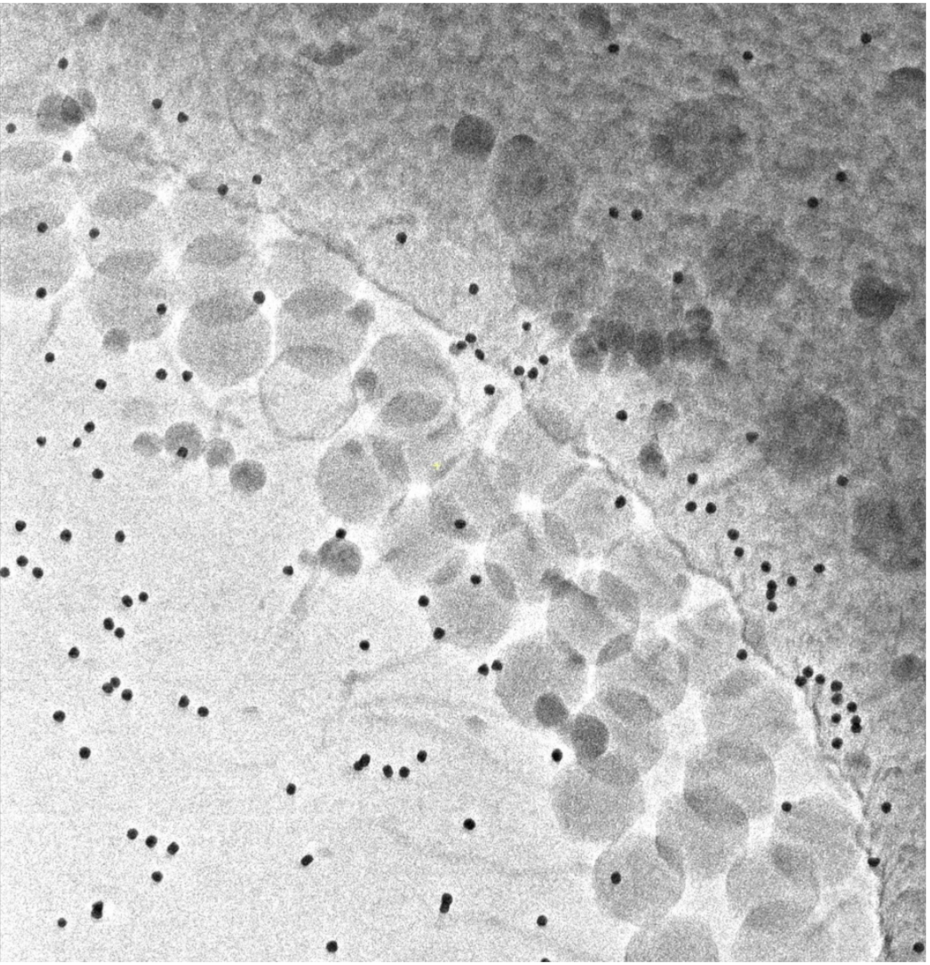

acquired series

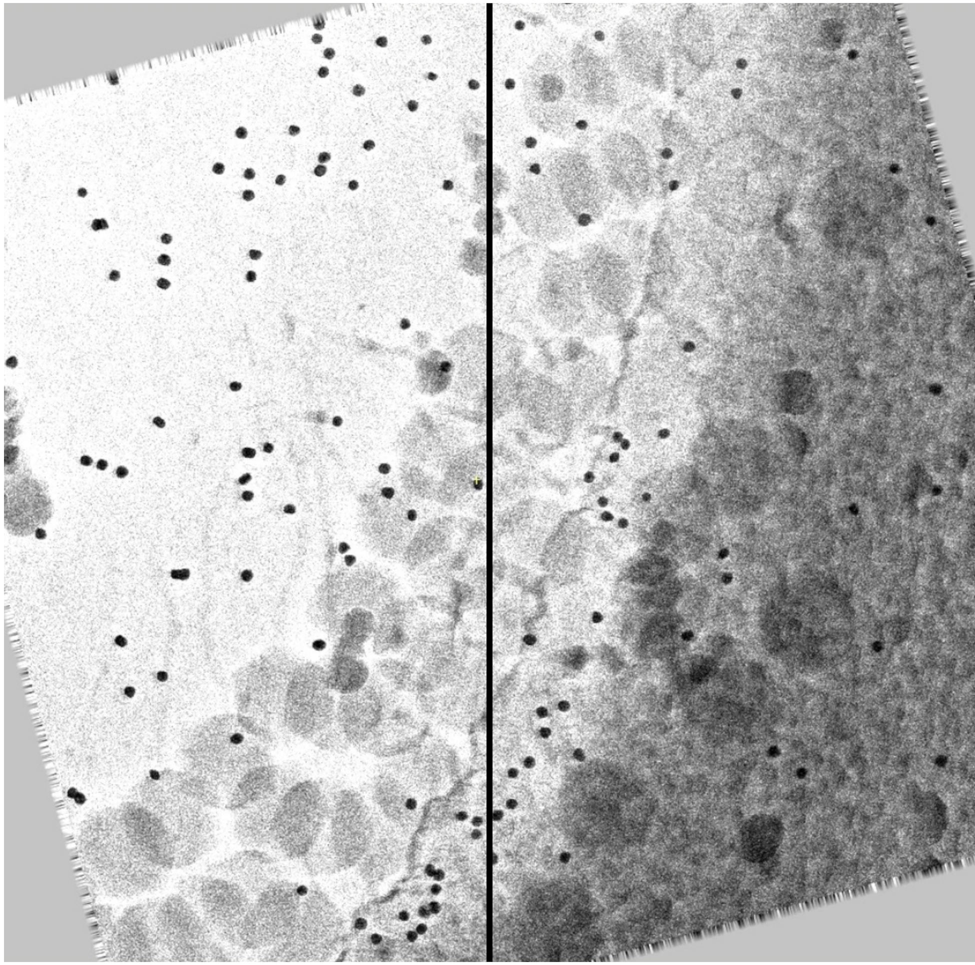

aligned series

Image alignment

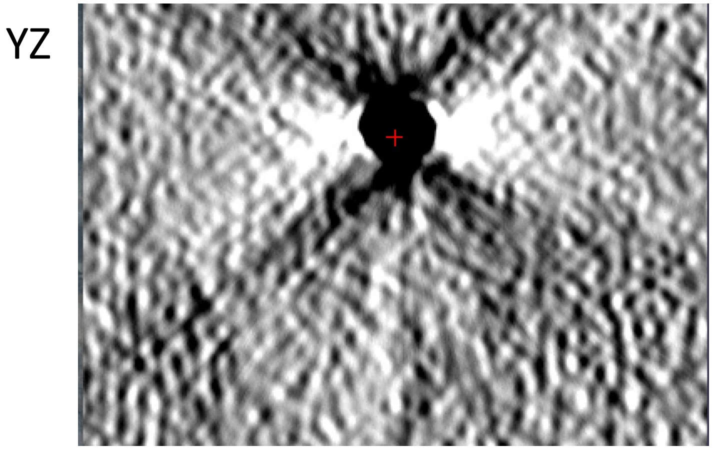

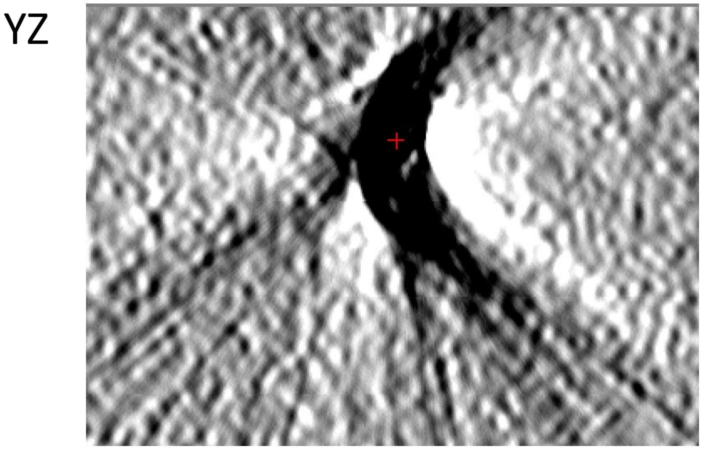

Alignment with fiducial markers

Alignment by simple correlation

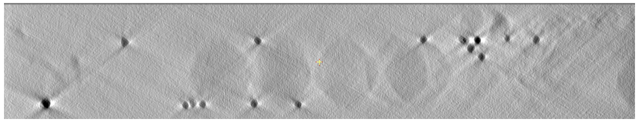

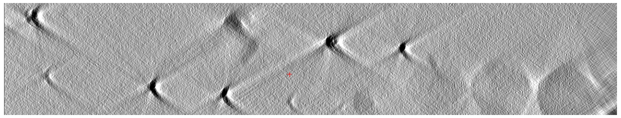

Tomogram reconstruction

Back Projection

Fourier space partially an inhomogeneously filled

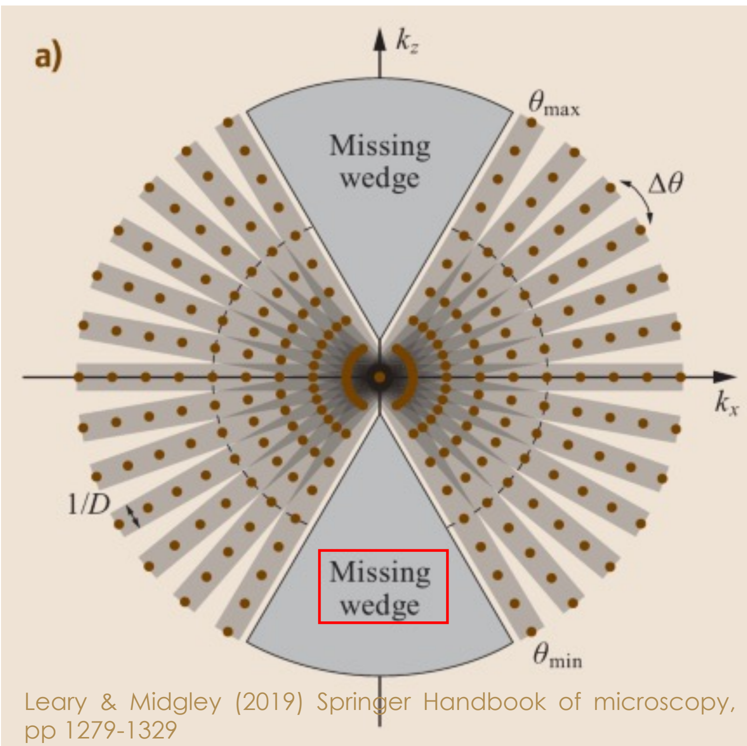

Leary & Midgley (2019) Springer Handbook of microscopy, pp 1279-1329

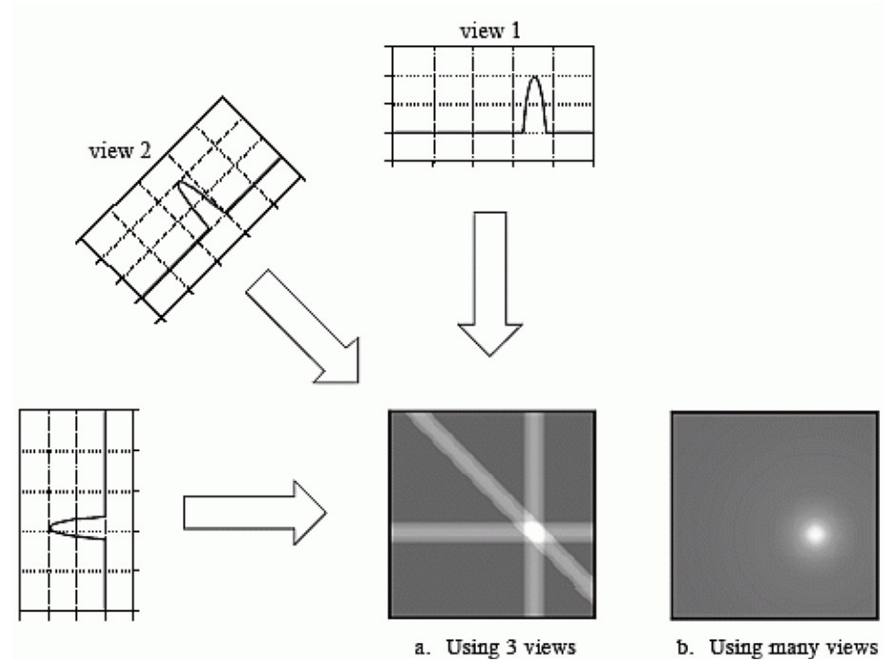

Smith (2011) Guide to Digital Signal Processing

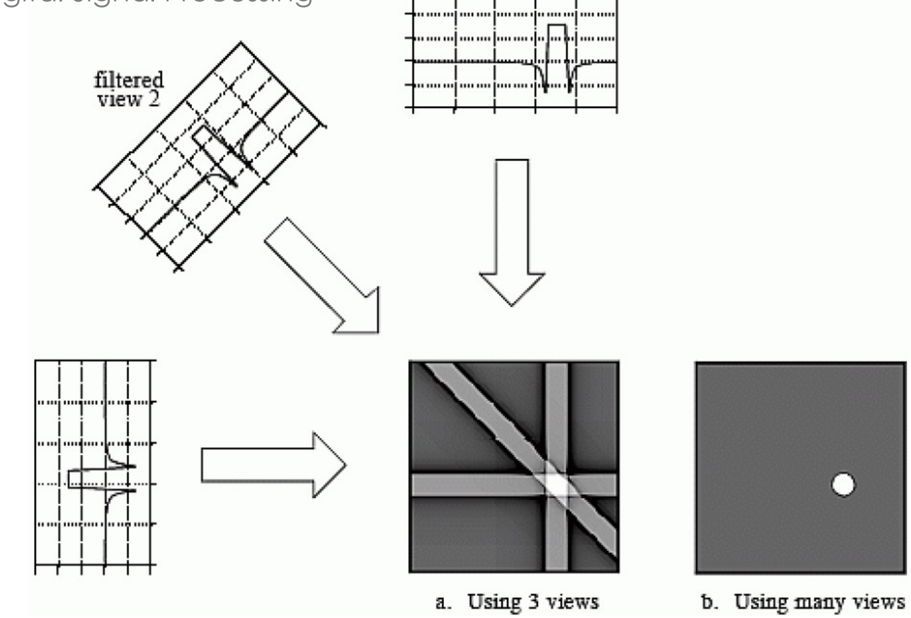

Weighted Back Projection (WBP)

Tomogram reconstruction

Algebraic iterative reconstruction methods

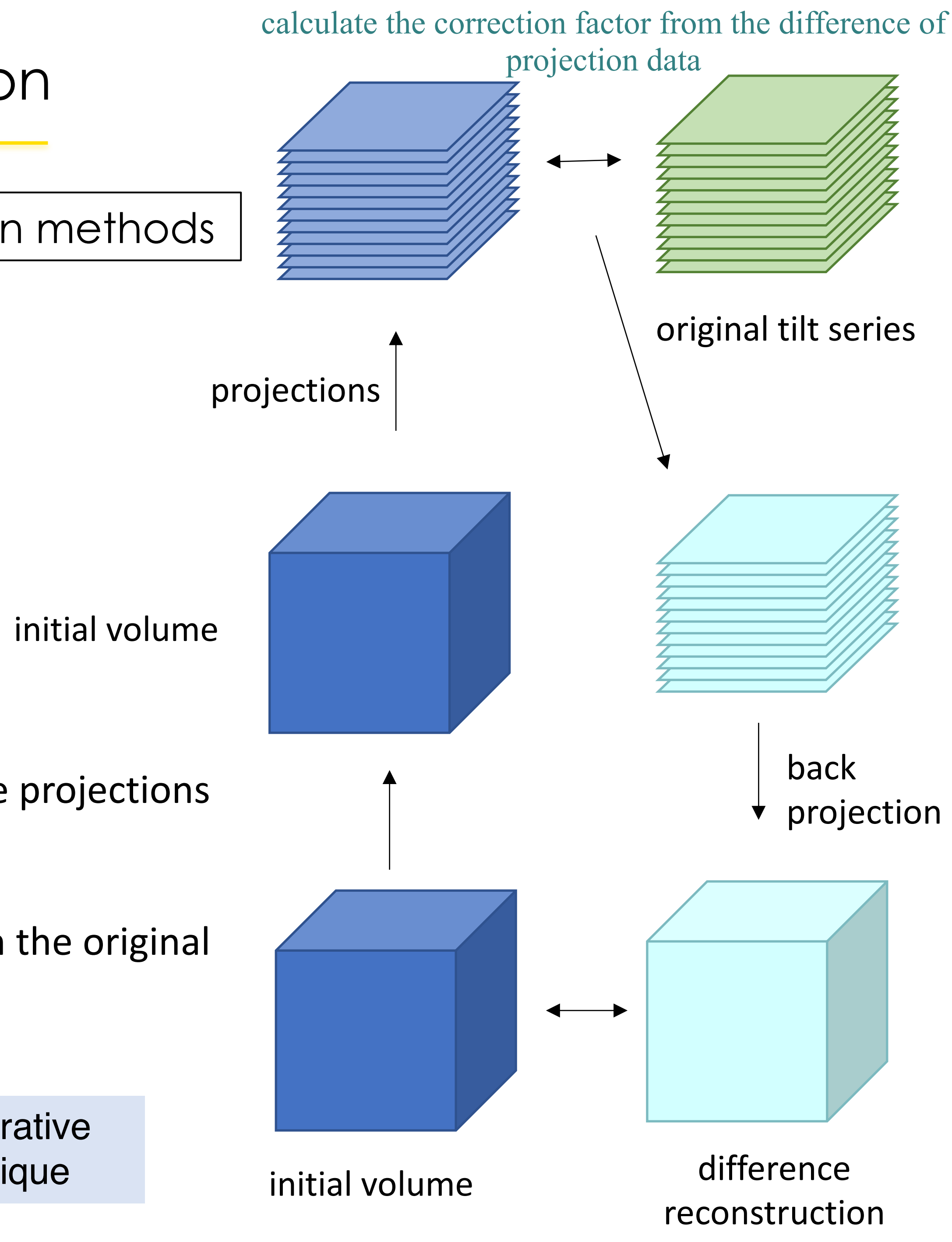

- minimize the differences between the projections from 3D and the 2D data
- improved by successive iterations
- constrain the reconstruction to match the original projections

SIRT: Simultaneous Iterative Reconstruction Technique

Tomogram reconstruction

Algebraic iterative reconstruction methods

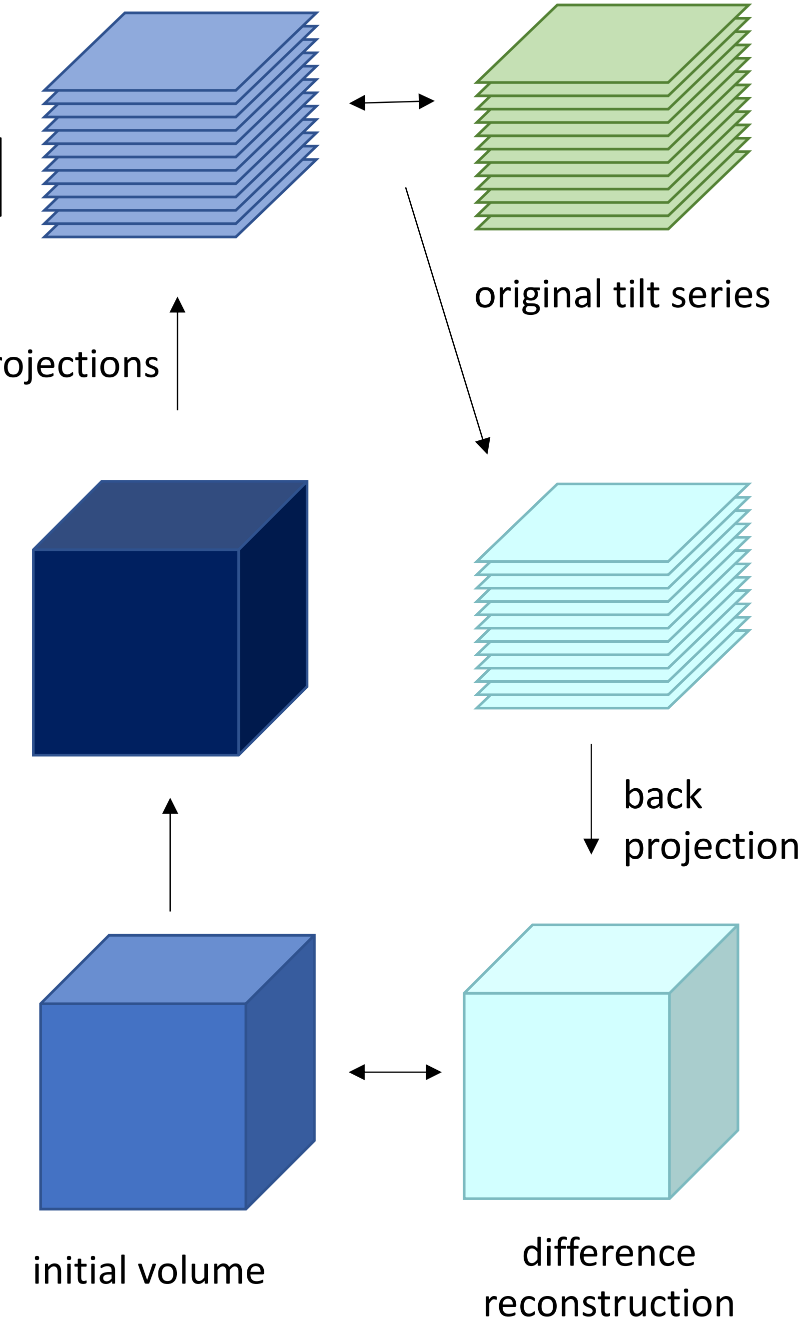

- minimize the differences between the projections from 3D and the 2D data
- improved by successive iterations
- constrain the reconstruction to match the original projections

SIRT: Simultaneous Iterative Reconstruction Technique

Tomogram reconstruction

Algebraic iterative reconstruction methods

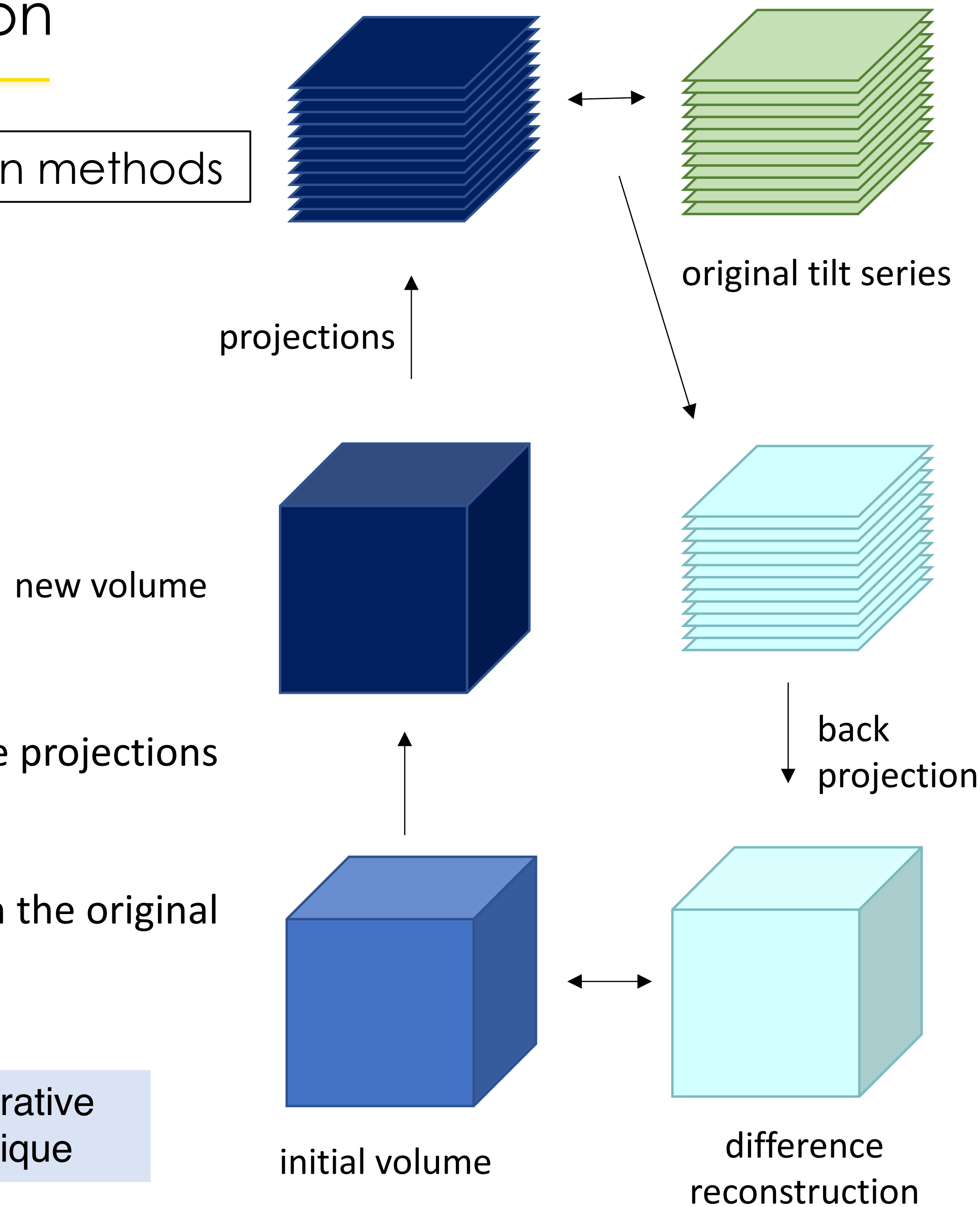

- minimize the differences between the projections from 3D and the 2D data
- improved by successive iterations
- constrain the reconstruction to match the original projections

SIRT: Simultaneous Iterative Reconstruction Technique

Tomogram reconstruction

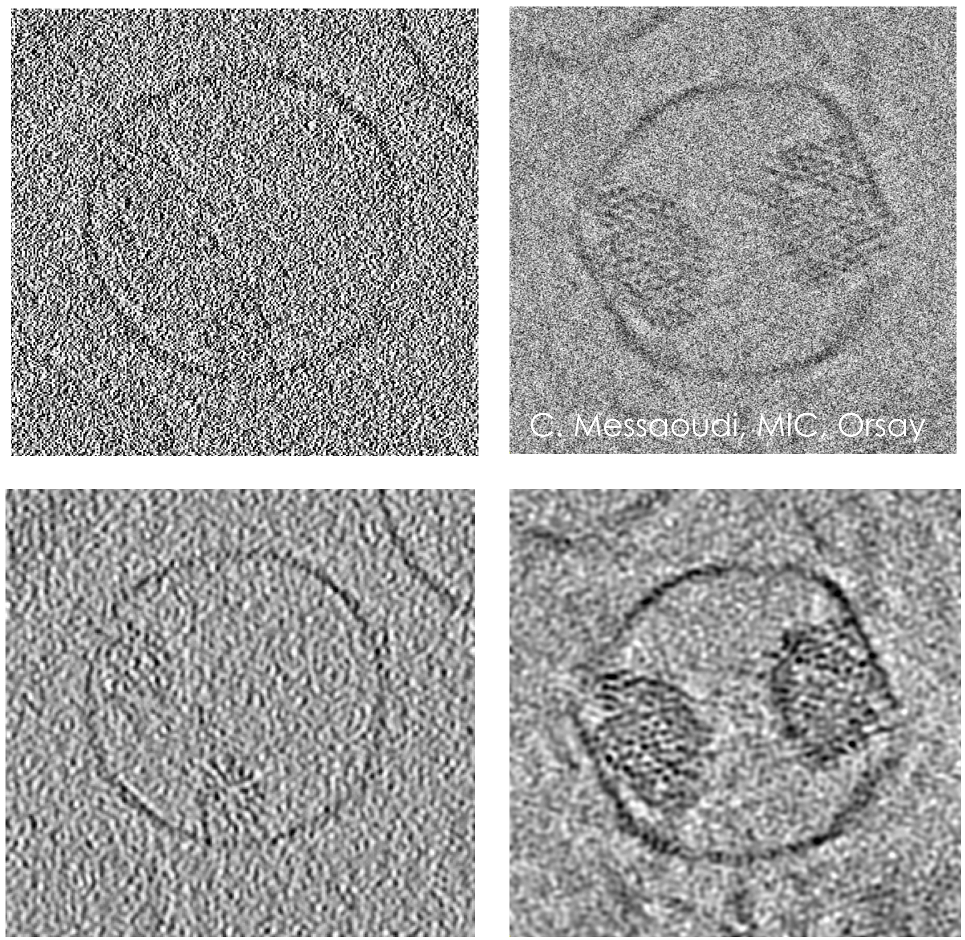

Virtual slices 0.218 nm

Tomogram visualisation

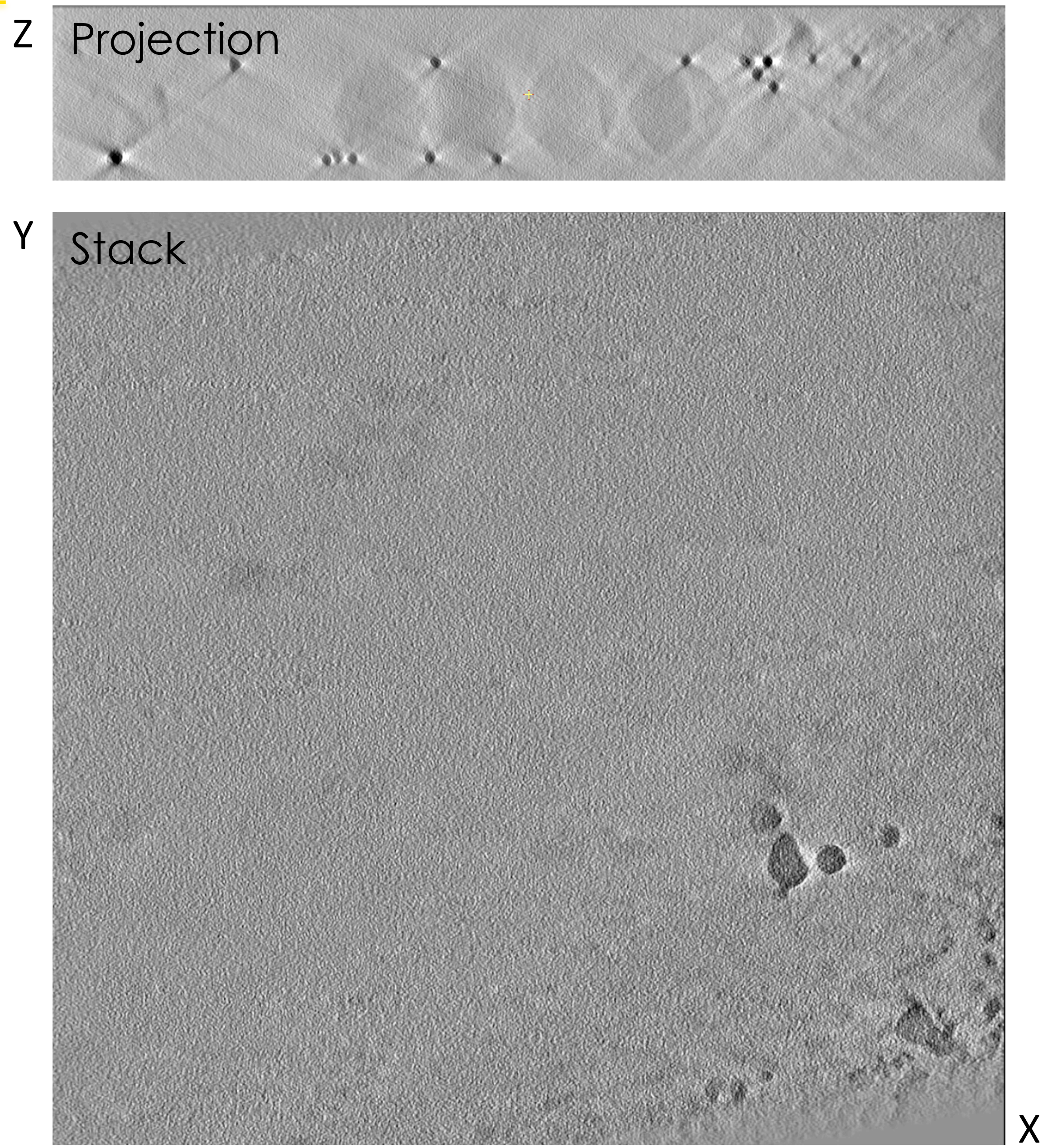

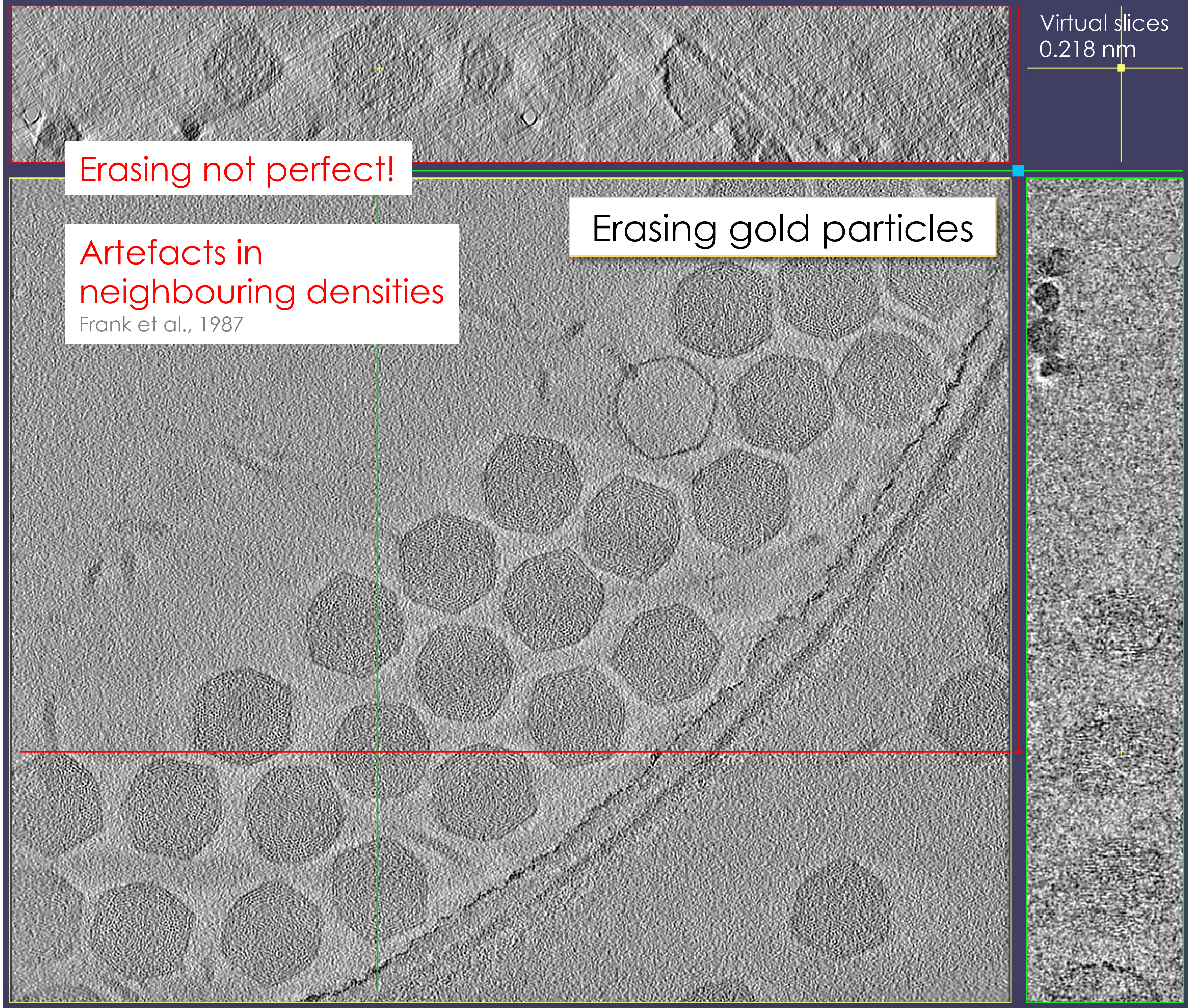
Virtual slices
0.218 nm
Erasing not perfect!
Artefacts in
neighbouring densities
Frank et al., 1987
Erasing gold particles

Tomogram visualisation

Virtual slices

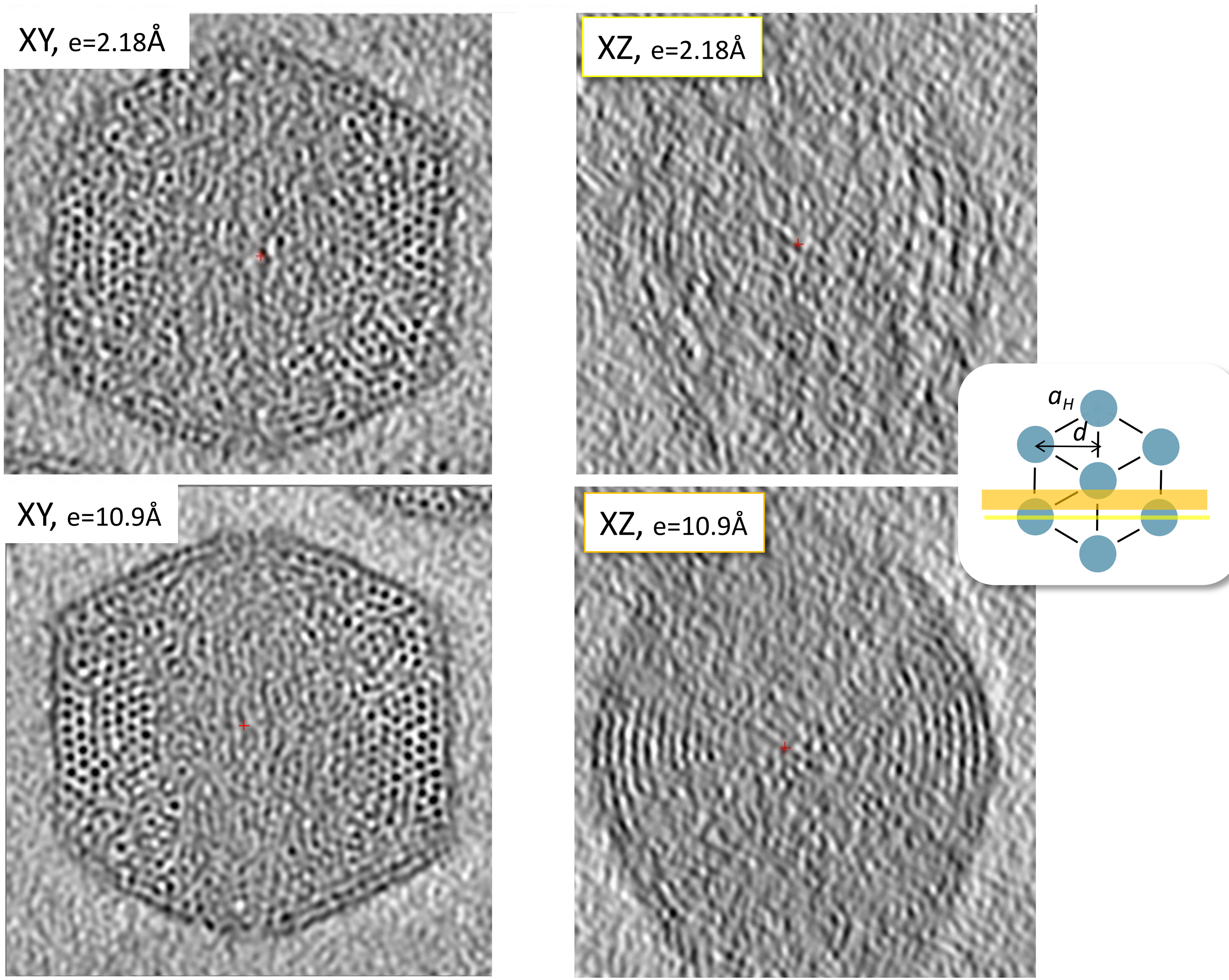

Tomogram visualisation

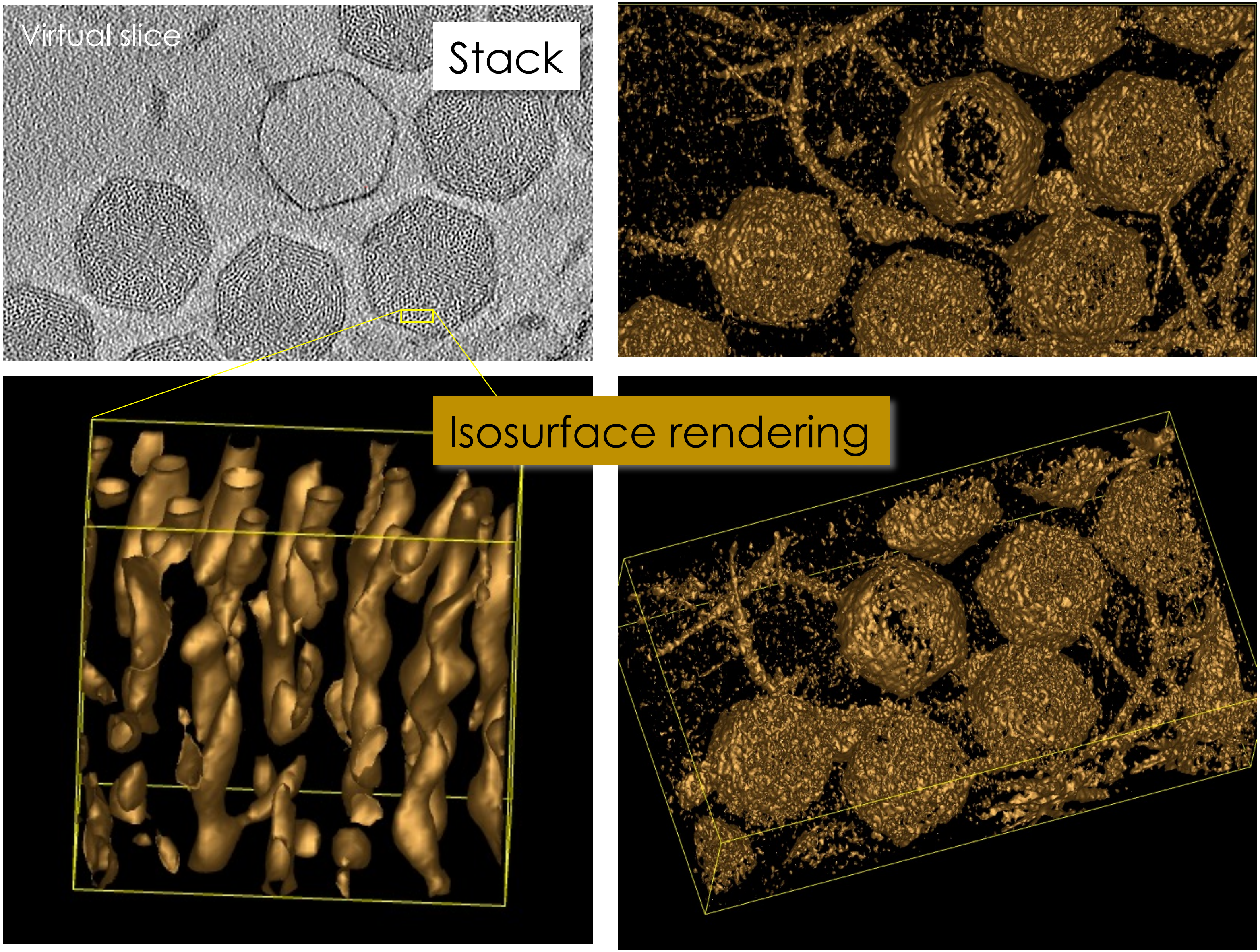

Softwares…

imod
Tom toolbox
SerialEM
UCSF Tomography
TomoJ
emClarity
M
W
Xmipp
Protomo
CTFFIND4
EMAN2
AreTomo
MBIR
NovaCTF
Dynamo
Relion
Chimera
…..

Tilt series acquisition
Motion correction
Tilt series alignment
CTF determination
CTF correction
Tomogram reconstruction
Particle picking
Subtomogram averaging

Conclusions & perspectives

- Missing information
- Tilt series acquisition
  (electron dose, acquisition schemes)
- CTF-correction (2D, 3D)
- Alignment
- Tomogram reconstruction
- Tomogram visualization
- Segmentation
- Sub-tomogram averaging (STA)

Denoising

Restauration of missing information

Cellular cryo-EM

A few references

• Chen M, Bell JM, Shi X, Sun SY, Wang Z and Ludtke SJ (2019) A complete data processing workflow for cryo-ET and subtomogram averaging. Nat Methods 16, 1161–1168.

• Penczek P, Marko M, Buttle K and Frank J (1995) Double-tilt electron tomography. Ultramicroscopy 60, 393–410.

• Turk, M., & Baumeister, W. (2020). The promise and the challenges of cryo-electron tomography. *FEBS letters*, *594*(20), 3243-3261.

• Wan, W. and Briggs, J.A.G., "Cryo-electron tomography and subtomogram averaging" (2016) Methods in Enzymology, 579, 329-367

• Pyle, E., & Zanetti, G. (2021). Current data processing strategies for cryo-electron tomography and subtomogram averaging. *Biochemical Journal*, *478*(10), 1827-1845.

• Danev R, Baumeister W. (2017) Expanding the boundaries of cryo-EM with phase plates. *Curr Opin Struct Biol.* 46:87-94. doi: 10.1016/j.sbi.2017.06.006.

• Tegunov, D., Xue, L., Dienemann, C., Cramer, P., & Mahamid, J. (2021). Multi-particle cryo-EM refinement with M visualizes ribosome-antibiotic complex at 3.5 Å in cells. *Nature Methods*, *18*(2), 186-193.

• Turoňová, B., Hagen, W. J., Obr, M., Mosalaganti, S., Beugelink, J. W., Zimmerli, C. E., ... & Beck, M. (2020). Benchmarking tomographic acquisition schemes for high-resolution structural biology. *Nature communications*, *11*(1), 1-9.

Grant Jensen's lectures https://www.youtube.com/playlist?list=PL8_xPU5epJdctoHdQjpfHmd_z9WvGxK8-